

**ANALİTİK UYGULAMALAR İÇİN İYON BASKILANMIŞ  
POLİMERİK KÜRELERE Fe<sup>3+</sup> ADSORPSİYONU**

169070

**ADSORPTION OF Fe<sup>3+</sup> ON ION IMPRINTED POLYMER  
BEADS FOR ANALYTICAL APPLICATIONS**

**ÖZGEN SAATÇILAR**

A THESIS OF MASTER OF SCIENCE  
Prepared In The Chemistry Department  
According To The Regulations of  
The Institute for Graduate Studies In Pure  
And Applied Science of Hacettepe University

ANKARA

2005

Graduate School of Natural and Applied Sciences,

This is to certify that we have read this thesis and our opinion it is fully adequate, in scope and quality, as **A Thesis for Degree of Master of Science in Chemistry.**

Chairman

.....S-Bektaş  
**Prof. Dr. Sema Bektaş**

Member

.....Kadir Pekmez  
**Prof. Dr. Kadir Pekmez**

Member

.....E. Gökoğlu  
**Prof. Dr. Elmas Gökoğlu**

Member (Supervisor)

.....N. Ögün Şatıroğlu  
**Assoc. Prof. Dr. Nuray Ögün Şatıroğlu**

Member

.....R. Say  
**Assoc. Prof. Dr. Ridvan Say**

#### APPROVAL

This thesis has been certified as a thesis for the Degree of Master by the above Examining Committee Members on ...../...../2005

...../...../2005

**Prof. Dr. Ahmet R. Özdural**  
Director of the Graduate School of  
Natural and Applied Sciences

.....

# ADSORPTION OF Fe(III) ON ION-IMPRINTED POLYMER BEADS FOR ANALYTICAL APPLICATIONS

ÖZGEN SAATÇILAR

## ABSTRACT

Iron is the fourth most abundant element in the earth's crust, it presents in a variety of rock and soil minerals both as iron(II) and iron(III). It plays an essential role in photosynthesis, and both iron(II) and iron(III) are important in the biosphere, serving as an active center of a wide range of proteins such as oxidases, reductases and dehydrases. Iron poisoning is rare. In an occupational setting, inhalation exposure to iron oxide may cause siderosis. In the nonoccupational population, ingestion of large quantities of iron salts may cause nausea, vomiting and intestinal bleeding. There is accumulating evidence suggesting that an increase iron storage may be associated with an increasing risk of developing cancer. Different metal complexing ligands carrying synthetic and natural adsorbents have been reported in the literature for heavy metal removal. We have used a novel and a new approach to obtain high metal adsorption capacity utilizing 2-methacryloylamidocysteine (MAC) as a metal-complexing ligand and/or comonomer. MAC was synthesized by using methacryloyl chloride and cysteine. In the first step, Fe<sup>3+</sup> was complexed with MAC monomer. Fe<sup>3+</sup>-imprinted p(HEMA-co-MAC) microbeads with average size of 150-200 µm were obtained by the suspension polymerization technique. After that, Fe<sup>3+</sup> ions were removed by 0.1 M HCl. Fe<sup>3+</sup>-imprinted p(HEMA-co-MAC) beads were characterized by swelling studies, FTIR and elemental analysis. The Fe<sup>3+</sup>-imprinted p(HEMA-co-MAC) beads with a swelling ratio of 72%, and containing 3.9 mmol MAC g<sup>-1</sup> were used in the removal of Fe<sup>3+</sup> ions from aqueous solutions, tap water, certified reference serum sample and real serum sample. The amount of metal was determined by using Flame Atomic Absorption Spectrophotometer (FAAS). Fe<sup>3+</sup>-imprinted p(HEMA-co-MAC) beads adsorption capacity, adsorption pH and adsorption time values were 107 µmol g<sup>-1</sup>, pH 3, 30 minutes, respectively. It was observed that even in the presence of other ions, Fe<sup>3+</sup>-imprinted p(HEMA-co-MAC) beads selectively adsorbed Fe<sup>3+</sup> ions with 97% efficiency and removal of Fe<sup>3+</sup> ions from certified reference serum sample was approximately found 33%.

**Key Words:** SPE, Ion-imprinting polymer, Fe<sup>3+</sup> removal.

**Supervisor:** Assoc. Prof. Dr. Nuray Ögün Şatıroğlu

# ANALİTİK UYGULAMALAR İÇİN İYON BASKILANMIŞ POLİMERİK KÜRELERE Fe<sup>3+</sup> ADSORPSİYONU

## ÖZGEN SAATÇILAR

### ÖZ

Demir yeryüzünde en bol bulunan dördüncü elementtir. Çeşitli kaya ve toprak minerallerinde Fe<sup>2+</sup> ve Fe<sup>3+</sup> formunda bulunur. Fotosentezde, oksidas, reduktans ve dehidras gibi pek çok proteinin aktif merkezlerinde hem Fe<sup>2+</sup> hem de Fe<sup>3+</sup> önemlidir. Demir zehirlenmesi çok karşılaşılan bir durum değildir. Mesleki koşullar gereği, solunum yoluyla alınan demir oksit siderosise neden olur. Yüksek miktarda demir tuzlarının sindirim yoluyla alınması mide bulantısına, kusmaya ve iç kanamaya sebep olabilir. Vücutta demir birikiminin kanser oluşma riskini arttırdığı öne sürülmektedir. Literatürde ağır metallerin uzaklaştırılması için değişik kompleksleştirici ligandlar içeren sentetik ve doğal adsorbentler verilmektedir. Bu çalışmada yüksek adsorpsiyon kapasitesine sahip 2-metakriloilamidosisistein (MAC) ligand ve/veya komonomer, metal kompleksleştirici olarak kullanılmıştır. MAC, metakriloil klorür ve sistein kullanılarak sentezlenmiştir. İlk basamakta, Fe<sup>3+</sup> iyonları MAC monomeriyle kompleksleştirilmiş, ortalama 150-200 µm büyüklüğe sahip Fe<sup>3+</sup>-baskılanmış p(HEMA-co-MAC) küreler süspansiyon polimerizasyon tekniğiyle sentezlenmiştir. Daha sonra Fe<sup>3+</sup> iyonları 0.1 M lik HCl çözeltisiyle uzaklaştırılmıştır. Fe<sup>3+</sup>-baskılanmış p(HEMA-co-MAC) kürelerin karakterizasyonunda şişme testi, FTIR ve elemental analiz yöntemleri kullanılmıştır. 3.9 mmol g<sup>-1</sup> MAC içeren ve şişme oranı 72% olan Fe<sup>3+</sup>-baskılanmış p(HEMA-co-MAC) küreler kullanılarak sulu çözeltilerden, çeşme suyu örneğinden, sertifikalı serum ve gerçek serum örneklerinden Fe<sup>3+</sup> iyonlarının uzaklaştırılması ile ilgili çalışmalar yapılmıştır. Deneylerdeki metal iyon miktarları Alevli Atomik Absorpsiyon Spektrofotometresi (FAAS) ile ölçülmüştür. Fe<sup>3+</sup>-baskılanmış p(HEMA-co-MAC) kürelerin adsorpsiyon kapasitesi, adsorpsiyon pH'ı ve adsorpsiyon zamanı sırasıyla 107 µmol g<sup>-1</sup>, pH 3 ve 30 dakika olarak bulunmuştur. Diğer metal iyonlarının varlığında bile Fe<sup>3+</sup>-baskılanmış p(HEMA-co-MAC) kürelerin Fe<sup>3+</sup> iyonlarını seçimli olarak adsorpladığı %97 oranında ortamdan uzaklaştırdığı bulunmuştur. Fe<sup>3+</sup> iyonlarının sertifikalı serum örneğinden uzaklaştırılma oranı %33 oranında bulunmuştur.

**Anahtar kelimeler:** Kati faz ekstraksiyonu, iyon baskılanmış polimerler, Fe<sup>3+</sup> uzaklaştırması.

**Danışman:** Doç. Dr. Nuray Ögün Şatıroğlu

## **ACKNOWLEDGEMENT**

First of all, I am very greatly indebted to Prof.Dr. Ömer Genç even though he is not near us, for his valuable guidance since the beginning of my academic studies.

With profound the respect and esteemed consideration, I would like to thank my supervisor Assoc. Prof. Dr. Nuray Öğün Şatirođlu, for her professional advice and constructive criticism and suggestion during my research.

Special thanks to Prof. Dr. Sema Bektaş for her suggestions and help during the experimental work.

I wish to thank Research Assist. Levent Soysal, Ayşenur Sağlam, Serhat Döker, İlkay Sökmen, Çiğdem Arpa, and İlknur Tokgöz, Murat Gelenođlu for their help in laboratory, for their collaborating, assisting and providing me a pleasant atmosphere to work in.

Also, I acknowledge with much thanks to my directors and my co-workers in Gemsan A.S. for their support and encouragement.

Finally, I am very much indebted to my fiancé İbrahim Sezgin and my family for their support, and encouragement during my M.Sc. studies.

## TABLE OF CONTENTS

	Page
ABSTRACT.....	i
ÖZET.....	ii
ACKNOWLEDGEMENT.....	iii
TABLE OF CONTENTS.....	iv
LIST OF FIGURES.....	vii
LIST OF TABLES.....	viii
1. INTRODUCTION.....	1
2. THEORETICAL.....	6
2.1. Trace Element Analysis in Waste-water and Biological Samples.....	6
2.2. Toxicological Profiles.....	8
2.2.1. Metals and/or metalloids toxic effects.....	8
2.2.2. Oxidative stress.....	10
2.2.3. Environmental effect.....	11
2.3. Determination of Metal Ions.....	12
2.3.1. Solid phase extraction.....	12
2.4. Atomic Absorption Spectrometry.....	15
2.4.1. Instrumentation.....	15
2.4.1.1. Radiation sources.....	16
2.4.1.2. Atomizers.....	16
2.4.1.3. Optics.....	18
2.4.1.4. Detectors.....	19
2.4.2. Interferences in atomic absorption spectrometry.....	19
2.4.2.1. Spectral interferences.....	19
2.4.2.2. Non-spectral interferences.....	20
2.5. Iron.....	21
2.6. Molecular Imprinting.....	24
2.6.1. Imprinting at surfaces.....	24
2.6.2. Applications.....	27
2.6.2.1. Separations.....	27

2.6.2.2. Sensors.....	28
2.6.2.3. Drug development and screening.....	28
2.6.2.4. Directed synthesis.....	29
3. EXPERIMENTAL.....	31
3.1. Materials.....	31
3.2. Preparation of Polymeric Beads.....	31
3.2.1. Synthesis of 2-methacryloylamidocysteine.....	31
3.2.2. Preparation of Fe <sup>3+</sup> - imprinted poly(HEMA-co-MAC) beads.....	32
3.2.3. Removal of the template (Fe <sup>3+</sup> ions).....	33
3.3. Characterization of Polymeric Beads.....	33
3.3.1. Surface area measurements.....	33
3.3.2. Swelling test.....	33
3.3.3. Elemental Analysis.....	34
3.3.4. FTIR Studies.....	34
3.4. Fe <sup>3+</sup> Ions Adsorption/Desorption Studies in Batch System.....	34
3.4.1 Reagents and apparatus.....	34
3.4.2 Selectivity experiments.....	35
3.4.3 Effect of interfering ions.....	37
3.5. Desorption and Reuse.....	37
3.6. Removal of Fe <sup>3+</sup> Ions from Tap-water and Certified Reference Serum.....	38
4. RESULTS and DISCUSSION.....	39
4.1. Properties of Polymer Beads.....	39
4.2. Adsorption of Fe <sup>3+</sup> and Fe <sup>2+</sup> Ions from Aqueous Solutions.....	43
4.2.1. Effect of pH.....	43
4.2.2. Equilibrium adsorption time.....	44
4.2.3. Adsorption Capacity.....	46
4.2.4. Competitive Adsorption.....	47
4.2.5. Interfering ions.....	49
4.2.6. Equilibrium studies.....	50
4.3. Desorption and Reuse.....	55
4.4. Removal of Fe <sup>3+</sup> Ions from Tap-water and Certified Reference Serum.....	56

5.	CONCLUSION.....	59
6.	REFERENCES.....	63
7.	CURRICULUM VITAE.....	74





## LIST OF FIGURES

	Page
<b>Figure 1.1.</b>	Molecular structure of Heme .....2
<b>Figure 2.1.</b>	Mechanisms of metal and metalloid toxicology.....9
<b>Figure 2.2.</b>	Possible interactions with in the elemental cycle between humans and their environment and mutual interactions between subdivisions of the environment..... 11
<b>Figure 2.3.</b>	Schematic representation of an atomic absorption spectrometer.....15
<b>Figure 2.4.</b>	Creating a molecular imprint in a synthetic polymer.....24
<b>Figure 2.5.</b>	Imprinting at surfaces.....25
<b>Figure 2.6.</b>	(a) Synthesis of a new ligand in the binding site of a MIP. (b) Synthesis of inhibitors of kallikrein.....30
<b>Figure 4.1.</b>	SEM micographs of Fe <sup>3+</sup> -imprinted p(HEMA-co-MAC) beads (A) surface; (B) cross-section.....40
<b>Figure 4.2.</b>	The molecular formula of MAC monomer.....41
<b>Figure 4.3.</b>	FTIR spectrum of MAC and MAC-Fe <sup>3+</sup> monomer.....41
<b>Figure 4.4.</b>	The molecular formula of p(HEMA-co-MAC) beads.....42
<b>Figure 4.5.</b>	(A) FTIR spectrum of pHEMA. (B) FTIR spectrum of Fe <sup>3+</sup> -imprinting p(HEMA-co-MAC)..... 42 beads.
<b>Figure 4.6.</b>	Effect of pH on Fe <sup>3+</sup> and Fe <sup>2+</sup> adsorption.....44
<b>Figure 4.7.</b>	Time dependent adsorption of Fe <sup>3+</sup> and Fe <sup>2+</sup> ions on the Fe <sup>3+</sup> -imprinting p(HEMA-co-MAC) beads.....45
<b>Figure 4.8.</b>	Adsorption capacity of Fe <sup>3+</sup> and Fe <sup>2+</sup> ion concentration on adsorption of metal ions on the Fe <sup>3+</sup> -imprinted poy (HEMA-co-MAC) beads..... 47
<b>Figure 4.9.</b>	The effect of NaCl, KCl, Mg(CO <sub>3</sub> ) <sub>2</sub> and Ca(NO <sub>3</sub> ) <sub>2</sub> on the adsorption of Fe <sup>3+</sup> ions on the Fe <sup>3+</sup> -imprinted p(HEMA-co-MAC) beads.....50
<b>Figure 4.10.</b>	Langmuir and Freundlich adsorption isotherms.....53
<b>Figure 4.11.</b>	Adsorption\Desorption cycle of Fe <sup>3+</sup> -imprinted p(HEMA-co-MAC) beads.....56

## LIST OF TABLES

	<b>Page</b>
<b>Table 2.1.</b>	Properties of flames.....17
<b>Table 2.2.</b>	The biological importance of iron exposure.....23
<b>Table 3.1.</b>	Recipe and polymerization conditions for the preparation of Fe <sup>3+</sup> -imprinted poly(HEMA-co-MAC) beads.....32
<b>Table 4.1.</b>	The effect of imprinting on selectivity.....48
<b>Table 4.2.</b>	Tolerance limit of interfering species.....49
<b>Table 4.3.</b>	Isotherm model constants and correlation coefficients for sorption of Fe <sup>3+</sup> ions.....54
<b>Table 4.4.</b>	Desorption agents for used Fe <sup>3+</sup> ions from the Fe <sup>3+</sup> -imprinted p(HEMA-co-MAC).....55
<b>Table 4.5.</b>	Removal of Fe(III) ions from tap water (N = 5).....56
<b>Table 4.6.</b>	Certified values of reference serum sample.....57
<b>Table 4.7.</b>	Removal of Fe <sup>3+</sup> ions in certified reference serum and real serum sample.....58

## 1. INTRODUCTION

Iron is one of the most abundant elements on earth. It makes up 4.7-5% of the earth's crust and 90% of the earth's core. Most iron ores are oxides or sulfides. Pure iron is a silvery-white, soft, ductile, malleable metal that is relatively reactive and that has high magnetic susceptibility.

Iron is used primarily in the production of steel. Iron and iron compounds are also used in the production of magnets, pigments, abrasives and polishing compounds. Iron is also released to the environment through recycling, waste incineration, and through the use of municipal sewage/sludge that contain iron. Nonoccupational exposure to iron occurs from contact with soil and from ingestion of plant and animal tissue.

The toxicity of iron is related to its ability to induce oxidative stress in cells (Strohs and Bagchi, 1995; Toyokuni, 1996). Iron poisoning is rare. In an occupational setting, inhalation exposure to iron oxide may cause siderosis. In the nonoccupational population, ingestion of large quantities of iron salts may cause nausea, vomiting and intestinal bleeding. There is accumulating evidence suggesting that an increase in iron storage may be associated with an increasing risk of developing cancer (Stevens et al., 1986; Stevens et al., 1988; Nelson et al., 1994; Stevens et al., 1994; Knekt et al., 1994). Studies have demonstrated that there is an increased risk for developing colorectal carcinoma following ingestion of high amounts of iron (Nelson, 1992). There is also an increase in hepatocellular carcinoma in patients with hereditary hemochromatosis, an inherited disorder in which there is hyperabsorption of iron from the intestinal tract, (Neidereau et al., 1985; Bradbear et al., 1985; Cotran et al., 1989; Hsing et al., 1995) and in lung cancer from exposure to asbestos fibers, which contains approximately 30% iron by weight (Mossman et al., 1990).

Iron exists in several valence states with the +2 ( $\text{Fe}^{2+}$ , ferrous) and +3 ( $\text{Fe}^{3+}$ , ferric) states being most important in biological systems. Iron is an essential element being involved in electron-transfer reactions, in photosynthesis, nitrogen fixation and respiration.

An average adult male contains 4.5 to 5 g of iron and absorbs about 1 mg per day in the diet (Crichton and Chaloteaux-Waters, 1987). Haemoglobin (BE) or hemoglobin (AE), is the iron-containing oxygen-transport metalloprotein in the red cells of the blood in mammals and other animals. The molecule consists of globin, the apoprotein, and four haem groups, an organic molecule with an iron atom.

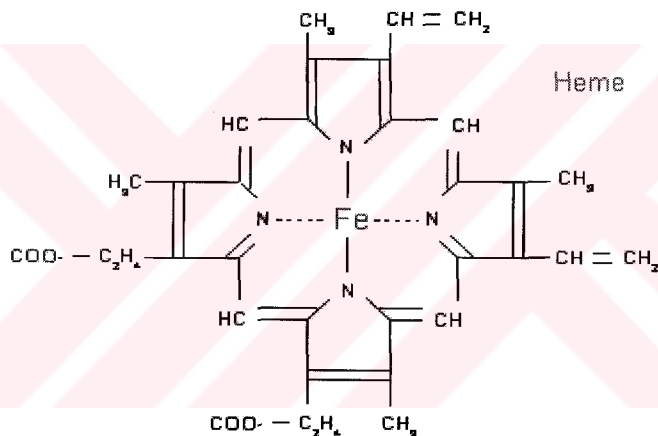


**Figure 1.1.** Molecular structure of Heme.

At the core of the molecule is a heterocyclic ring, known as a porphyrin which holds an iron atom; this iron atom is the site of oxygen binding. An iron containing porphyrin is termed a heme. The name *hemoglobin* is the concatenation of *heme* and *globin*, a globin being a generic term for a globular protein. Since a single subunit of hemoglobin is, in fact, made of a heme imbedded in a globular protein, the name makes sense. There are a number of heme containing proteins. Hemoglobin is by far the best known.

In plasma, the major iron transport protein, transferrin, binds iron (ferric,  $\text{Fe}^{3+}$ ) at a stoichiometry of 2:1. Uptake of the  $\text{Fe}^{3+}$ -transferrin complex occurs primarily by

receptor-mediated endocytosis, using the transferrin receptor (Crichton and Chaloteaux-Waters, 1987). Lactoferrin, a protein that is similar to transferrin in that it binds  $\text{Fe}^{3+}$  at a stoichiometry of 2:1, is found in milk and it is produced by phagocytes. A small proportion of iron may enter cells as nontransferrin bound iron (Crichton and Chaloteaux-Waters, 1987; Wright et al., 1988) and into hepatocytes as heme. Once internalized, iron is released from transferrin, which recycles to the membrane and reenters the circulation. Intracellular  $\text{Fe}^{3+}$  binds to ferritin, the major iron storage protein (Crichton and Chaloteaux-Waters, 1987; Seligman et al., 1987). Ferritin acts as a protein shell that surrounds an iron core; a molecule of ferritin can contain 4500 ions of iron. Ferric iron, when required for cellular functions is released from ferritin by reducing agents such as ascorbic acid, cysteine, glutathione and thioredoxin (Crichton and Chaloteaux-Waters). Ferritin has a half life of approximately 24 hours and the degradative product, hemosiderin, accumulates in lysosomes (Ramm et al., 1994). Iron is eliminated in the feces (turnover of intestinal epithelium), perspiration and urine.

For the determination of iron species in various samples, the techniques such as complexation with specific chelating reagent followed by spectrophotometric measurement (Singh, 1999) (Sarma et al., 2000) (Akl, 2003), potentiometry and ion-exchange voltammetry at ionomer-coated electrodes (Ugo et al., 2002), the preconcentration/separation by adsorption-atomic absorption determination, chelating resins usage for iron detoxification of human plasma (Feng et al., 1994) were generally used. Finally, Pehkonen reviewed the methods used for determination of iron in different oxidation state (Pehkonen, 1995). Although, 1-(2-pyridylazo)-2-naphthol (PAN) has been used for determination of iron using spectrophotometry (Shibata, 1961) (Taher and Krishan, 1995), the other ions can interfere and very effort should be consumed to overcome these undesired effects.

It has been a long term dream of researchers to build such structures de novo, creating tailor-made receptors that are capable of recognizing and binding the

desired molecular target with a high affinity and selectivity. Such synthetic materials should be easier to produce and process, less costly, and more stable than biomacromolecules. Moreover, they should be accessible to target molecules for which natural receptors do not exist are difficult to obtain. One surprisingly simple way of generating artificial macromolecular receptors is through the molecular imprinting of synthetic polymers (Søllergren, 2001; Komiyama, 2002).

Molecular imprinting is a method to introduce molecular recognition sites into polymeric materials. In other words, the molecular memory, which is both the shape of the target molecule and alignment of the functional moieties to interact with those in the target molecule, are memorized in the polymeric materials for the recognition or separation of target molecule during formation of the polymeric materials themselves (Yoshikawa, 2002).

In this thesis, ion-imprinted polymer beads were prepared and they were used for the selective separation of  $\text{Fe}^{3+}$  ions from complex matrices. Methacryloylamidocysteine (MAC) was synthesized as the metal complexing monomer by template polymerization, with the goal preparing a solid-phase which has the high selectivity for  $\text{Fe}^{3+}$ . Usually, molecularly imprinted polymers are prepared by the bulk polymerization method. The disadvantage of this method is that the obtained block polymers should be crushed, ground and sieved to produce packing materials. But in this study,  $\text{Fe}^{3+}$ -imprinted poly(hydroxyethyl-methacrylate-methacryloylamidocysteine) beads were produced by a dispersion polymerization. PHEMA was selected as the basic polymer matrix which has hydrophilic character, minimal non-specific protein interactions, high chemical and mechanical stability and resistance toward microbial and enzymatic attacks (Denizli, 1999) (Horbett and Brash, 1987). After removal of  $\text{Fe}^{3+}$  ions,  $\text{Fe}^{3+}$ -imprinted beads were used for the separation of iron from complex matrices.  $\text{Fe}^{3+}$  adsorption on the  $\text{Fe}^{3+}$ -imprinted beads from complex matrices containing different amounts, and selectivity studies of iron versus other

interfering metal ions mixture which  $\text{Fe}^{2+}$ ,  $\text{Cr}^{3+}$ ,  $\text{Cu}^{2+}$  and  $\text{Zn}^{2+}$  were reported here. Finally, use of the  $\text{Fe}^{3+}$ -imprinted p(HEMA-co-MAC) beads in tap water and certified reference serum sample was also discussed.



## **2. THEORETICAL**

### **2.1. Trace Element Analysis in Waste-water and Biological Samples**

Water analysis includes the investigation of drinking water, fresh waters and sea-water, and also sediments.

The analyte metals are generally already present in solution and it thus only necessary to select a technique of sufficient sensitivity for the analysis. The concentrations of dissolved substances in fresh waters are generally so low that apart from ionization, no major interferences for the determination of the alkali metals are to be expected. As long as the concentrations of the analyte elements are sufficiently high, or the sensitivity of flame AAS adequate, the metal salts dissolved in water can be determined directly without preparation. For natural waters this is principally valid for sodium, potassium, calcium and magnesium and also frequently for zinc. The most important trace elements, copper, iron, cobalt, nickel, manganese and chromium, on the other hand, usually can not be determined with the required sensitivity by the direct method. Generally a preconcentration procedure or the use of graphite furnace technique is necessary.

The most frequently employed preconcentration procedure in water analysis for trace elements is complexing the metal ions with ammonium pyrrolidine dithiocarbamate (APDC) and subsequently extracting into methyl isobutyl ketone (MIBK). This extraction system has the advantage that relatively stable chelates are formed with numerous metals over a wide pH range, so that with a single extraction the majority of trace elements can be simultaneously extracted. Using this procedure, many authors successfully extracted and subsequently determined copper, zinc, iron, cobalt, nickel, lead, manganese and other elements. Joyner and Finley complexed iron and manganese in sea-water with sodium diethyl dithiocarbamate and extracted the complex MIBK (Joyner and Finley, 1966). Vanderborcht and Van Grieken combined chelation with 8-hydroxyquinoline and preconcentration on activated charcoal for the determination of trace elements in



natural water (Vanderborcht and Van Grieken, 1997). Hall and Godinho found that freeze drying of natural waters for the determination of aluminium, cadmium, chromium, copper, iron, manganese, and nickel was just as effective as extraction or enrichment on an ion-exchange column (Hall and Godinho, 1980).

Also, the analysis of particulate matter and sediments will be discussed briefly as it is occasionally associated with water analysis. The sediment fraction is usually digested in one of the common acid mixtures and, after dilution, is analyzed by the flame technique (Anderson, 1974) (Bukenberg et al., 1972) (Forstner and Muller, 1974). Shock and Mercer found that using less sensitive resonance lines for iron, copper and manganese saved a good deal of time compared to making the usual dilutions. They found no deterioration in the accuracy and precision, while there were fewer errors and less risk of contamination (Shock and Mercer, 1977). Losser determined iron in nitric acid extracts of sediments from the continental shelf (Losser, 1978).

While tissue samples, for obvious reasons, must be wet or dry ashed before the analysis, iron, copper and zinc can frequently be determined in serum. Zinc is easiest to determine because of its high sensitivity (Ringhardt and Welz, 1968); it can be determined directly against aqueous reference solutions without interferences in 1:5 diluted serum and undiluted or 1:2 diluted urine (Reinhold et al., 1968). The determination of copper and iron in serum presents greater problems because of the low sensitivities of these two elements. Owing to the relatively high viscosity of blood serum, it cannot be compared with aqueous reference solutions; on the other hand higher dilutions considerably worsen the sensitivity and precision of the determination. For this reason, various authors have recommended deproteinization (Berman, 1965), (Tavenier and Hellendoorn, 1969), (Campenhausen and Muller-Plathe, 1975) or extraction (Parker et al., 1967), (Zettner et al., 1966), which however is somewhat time consuming for routine determinations. Olsen and Hamlin (Olsen and Hamlin, 1968) recommended a simple deproteinization procedure with which 95% of the hemoglobin iron can be removed

at the same time. Atomic absorption spectrometry also serves ideally for the determination of the iron binding capacity (Olson and Hamlin, 1969), (Zaion, 1967), (Zettner, 1966) and iron in hemoglobin (Herrmann et al., 1965), (Bokowski, 1968), (Zettner and Mensch, 1968). Increasingly, tissue samples, especially liver tissue, are being examined by AAS for their content of iron, copper and zinc (Johnson, 1976), (Evenson and Anderson, 1975).

## **2.2. Toxicological Profiles**

The adverse effects of metals and metalloids on human health are well documented. There have been numerous studies performed, using different model systems, to determine the effects that metal and metalloids have on biological processes and to relate these effects to clinical syndromes. These studies have contributed greatly to our understanding of the toxic effects that metals and metalloids have on biological processes. The majority of these studies were performed using acute exposure models in which cells or organisms are exposed to relatively toxic concentrations of metals or metalloids. Acute exposure to toxic concentrations of these environmental pollutants is not likely to occur in today's environment. Instead most human populations are chronically exposed to concentrations of metal and metalloid ions that are below the threshold levels associated with the development of clinical symptoms. Concerns have been raised about the health risks associated with such exposures (Lave, 1990).

### **2.2.1. Metals and/or metalloids toxic effects**

Metal and metalloids exert their toxic effects in biological systems through many different mechanisms (Figure 2.1). Nonessential metal ions may replace naturally occurring metal ions in cellular macromolecules. Metal ions also bind to a variety of chemical groups, i.e. amino, carboxyl, endiol, imidazole, phosphoryl, and this may alter the ability of the macromolecule to function in biological processes. Metal and metalloid ions, such as arsenic, cadmium, lead and mercury, have a high affinity for sulfhydryl residues present in proteins and small molecular weight thiols.

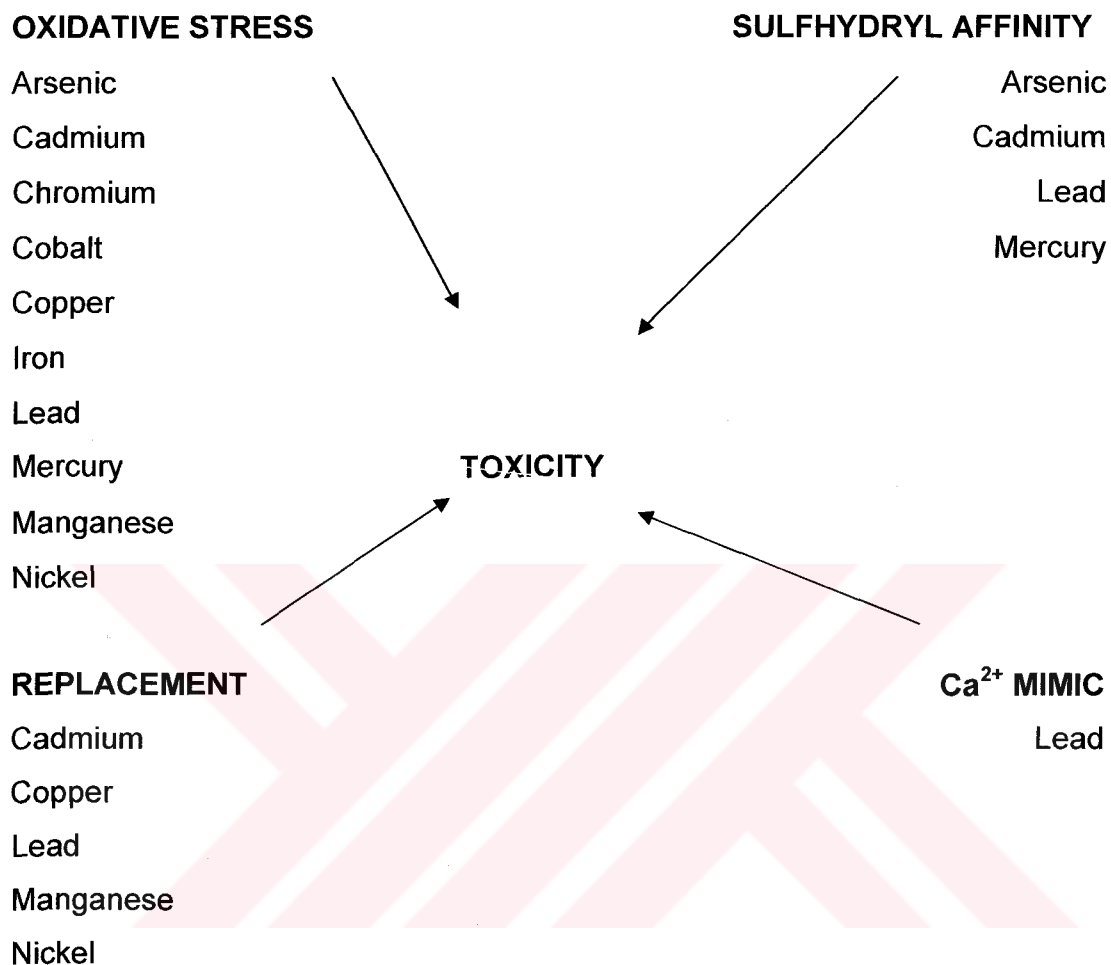


**Figure 2.1.** Mechanisms of metal and metalloid toxicology.

Depletion of small molecular weight thiols, such as glutathione, alters the redox status of a cell and this promotes oxidative damage. Likewise, metals may bind to metal-binding regions in enzymes that are important for biological functions, including anti-oxidant protection. Inhibition of these enzymes also results in oxidative stress. Some transition metals participate directly in the production in reactive oxygen species, which induce oxidative damage to cellular macromolecules. There are many reports in the literature that attribute the toxicity of a particular metal or metalloid to a single property. For example, since  $Pb^{2+}$  has a high affinity for

sulfhydryl residues in proteins, it has been proposed that the toxicity of  $Pb^{2+}$  is due to its ability to act as a non-specific enzyme inhibitor. However,  $Pb^{2+}$  also forms stable complexes with oxygen and nitrogen groups in macromolecules, it is a calcium mimic and it causes oxidative stress in cells even though its not a transition metal (Habermann et al., 1983; Lawton and Donaldson, 1991; Donaldson and Knowles, 1993; Ariza et al., 1998). Exposure to low concentrations of metal and metalloid ions results in less than 40% of the cell in the population being killed. Using this guidelines, the cytotoxicity of  $Pb^{2+}$  at high concentrations, reflects its ability to inhibit biological processes by multiple mechanisms and under these conditions of exposure, toxicity does not equate to cell death. Cellular damage is occurring, but the cell is either capable of repairing the damage or it can tolerate the damage and survive. Thus, the toxicity of a metal or metalloid ion is determined by its physicochemical properties, the duration, concentration and route of exposure, biological factors that modulate bioavailability, and the ability to affect multiple biological processes by different mechanism.

### **2.2.2. Oxidative stress**

Low quantities of reactive oxygen intermediates (ROIs) and reactive oxynitrogen intermediates (RONIs) are required for normal cellular functioning. However, the enhanced production of radicals and oxidants results in oxidative stress which is detrimental to a cell's survival. Metals and metalloids constitute a major group of environmental pollutants that are potentially toxic to humans. One mechanism by which metal and metalloid ions exert toxicity by inducing oxidative stress. Arsenic, cadmium, chromium, cobalt, copper, iron, lead, manganese, mercury, nickel and zinc include oxidative stress in cells, but by different mechanisms.

Metal ions are not free in solution, but rather they are complexed to other molecules. Cellular proteins provide many metal binding sites, i.e. amine, thiol and carboxyl groups, that act as ligands in potential metal-binding sites. The general order of divalent metal binding to these sites is  $Cu^{2+} > Zn^{2+} > Ni^{2+} > Co^{2+} > Fe^{2+} > Mn^{2+} > Mg^{2+} > Ca^{2+}$ . However, since metals ions have low ligand specificity and a high affinity for

many chemical groups, they bind to many macromolecules, particularly nucleic acids and proteins.

### 2.2.3. Environmental effect

The general term environmental covers a whole range of factors that influence our lives. It is hardly possible to pick out any specific area and regard this in isolation since all factors influence each other mutually. In Figure 2.2. the complex environmental relationships are depicted in simplified form and possible interactions indicated.

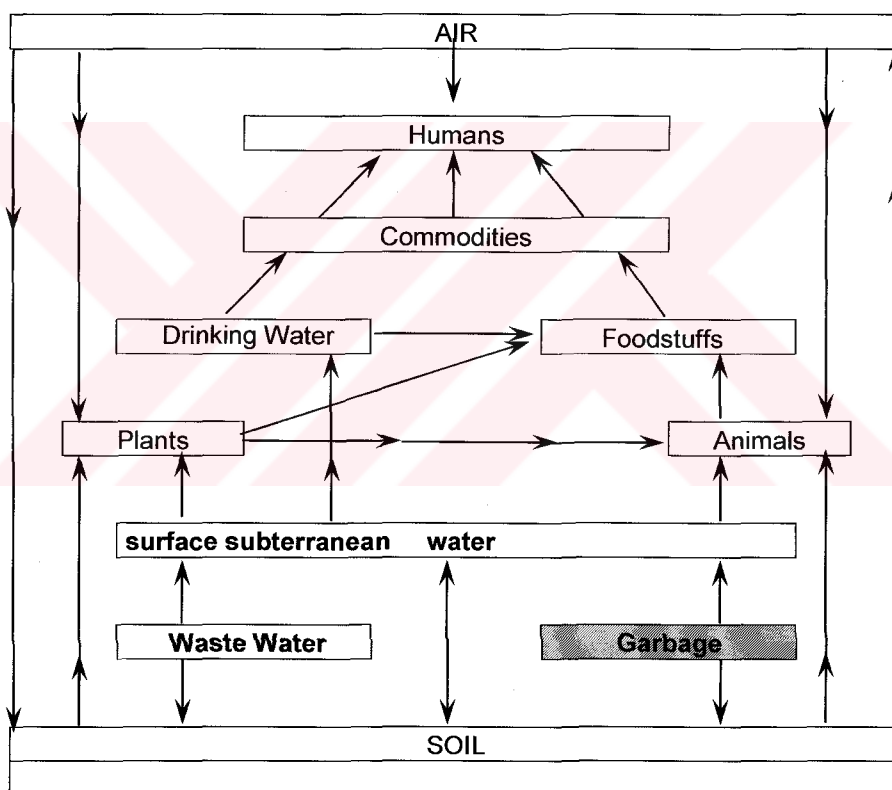


**Figure 2.2.** Possible interactions with in the elemental cycle between humans and their environment and mutual interactions between subdivisions of the environment (Aurand, K.).

Metals and their compounds are among the most insidious pollutants of our environment because they are not biologically degradable. Only a very few metals

are nontoxic, even at high concentration; a large number are very active and even at very low concentrations cause changes in humans, animals and plants. Removal of metals from natural cycles is usually only possible via the formation of insoluble or inactivate compounds and sediments. Even in these forms they are a potential source of danger, since they can be mobilized through the action of microorganisms or a change of pH, for example. Metals in the environment can originate from natural sources or as a result of human activity.

### **2.3. Determination of Metal Ions**

Trace heavy metal analysis are an important part of studies in analytical chemistry. The determination of these ions in the various samples have been performed continuously (Purves, 1985) (Minezevski et al., 1982) (Soylak et al., 1997) (Saraymen and Soylok, 1997). Due to the matrix effects and low metal levels in atomic absorption spectrometry, preconcentration/separation methods (Namboothiri et al., 1991) (Kubova et al., 1994) (Turker et al., 1997) (Soylak, 1998) (Saracoglu et al., 2001) (Silva et al., 2001) including extraction, coprecipitation, ion exchange and solid phase extraction procedures are a necessity for the determination of the traces metal ions in the highly saline media.

#### **2.3.1. Solid phase extraction**

Solid phase extraction (SPE) is a method of sample preparation that concentrates and purifies analytes from solution by sorption onto a disposable solid phase cartridge, followed by elution of the analyte with a solvent appropriate for instrumental analysis. Traditionally, sample preparation consisted of sample dissolution, purification, and extraction that were carried out with liquid-liquid extraction (LLE). The disadvantages with LLE include the use of large volumes of organic solvent, cumbersome glassware, and cost (Thurman and Mills, 1998). SPE is replacing LLE due to the following advantages of the former technique. This includes (Junker-Bunchheit and Witzenbacher, 1996), (Pyrzynska and Trojanowicz, 1999), (Glaidis and Rao, 2002), (Rao and Preetha, pers. commun.):

- (I) higher enrichment factors,
- (II) absence of emulsion,
- (III) safety with respect to hazardous sample,
- (IV) minimal costs due to low consumption of reagents,
- (V) flexibility,
- (VI) incorporation into automated analytical techniques.

As a result of the flexibility that SPE offers, it has found application in the preparation of environmental, clinical, and pharmaceutical samples. Examples include the concentration of trace organic pollutants from water, the purification of drugs of abuse from blood and urine, and the extraction of organic compounds from food and beverages.

The sorbents used for SPE are similar to those used in liquid chromatography, including normal phase, reversed phase, size exclusion (commonly called wide pore), and ion exchange.

Normal-phase sorbents consist of a stationary phase that is more polar than the solvent or sample matrix that is applied to the SPE sorbent. Normal-phase sorbents, therefore, are used in SPE when the sample is an organic solvent containing an analyte of interest. Polar interactions, such as hydrogen bonding and dipole-dipole interactions are the primary mechanisms for solute retention.

Reversed-phase sorbents are packing materials that are more hydrophobic than the sample. Reversed-phase sorbents are commonly used in SPE when aqueous samples are involved. The mechanism of interaction is van der Waal's forces (also called nonpolar, hydrophobic, or reversed-phase interactions) and occasionally secondary interactions such as hydrogen bonding and dipole-dipole interactions.

Size-exclusion sorbents utilize a separation mechanism based on the molecular size of the analyte. It is a method only recently being used in SPE, usually in conjunction with reversed phase or ion-exchange.

Ion-exchange sorbents isolate analytes based on the ionic state of the molecule, either cationic or anionic, where the charged analyte exchanges for another charged analyte that already sorbed to the ion-exchange resin. Solid phase extraction applications in this case are essentially identical to classical ion exchange.

Thus the mechanisms of interaction include hydrogen bonding and dipole-dipole forces (polar interactions), van der Waal's forces (nonpolar or hydrophobic interactions), size exclusion, and cation and anion exchange.

Some sorbents combine several interactions for greater selectivity. The extensive line of sorbent chemical structure facilitates one of the most powerful aspects of SPE, that is, selectivity. Selectivity is the degree to which an extraction technique can separate the analyte from interferences in the original sample. The number of possible interactions between the analyte and the solid phase facilitates selectivity (Thurman and Mills, 1998).

Hence, much of the current research in selecting sorbents in SPE, is use of the molecular imprinting materials (MIP) (Haupt, 2001) due to their low price and stability in different environments and also more selective than common solid sorbents such as immobilized naphthalene, cellulose, C<sub>18</sub> bonded silica membrane discs, silica gel, glass beads, silica frit, metal hydroxides, activated carbon and functionalized polymer supports for preconcentrative separation of trace and ultra trace metal ions.

The application of molecular imprinting in the analytical separation field most close to practical realization is probably that of solid phase extraction, SPE. Several groups have already applied MIP-based solid phase extraction to biological and



environmental samples and this technique may well be accepted generally in the not-to-distant future. The technique has variously been referred to as MIP-SPE or MIPSPE and has been reviewed recently (Olsen et al., 1998), (Andersson, 2000).

## 2.4. Atomic Absorption Spectrometry

The principal aim of a quantitative analysis is to determine the analyte content in an unknown sample with good trueness and precision, i.e. with high accuracy. In practice, however, this aim is unfortunately made difficult by a variety of problems that are more or less associated with every analytical method. Atomic Absorption Spectrometry (AAS) is the measurement of the absorption of optical radiation by atoms in the gaseous state.

### 2.4.1. Instrumentation

The general construction of an atomic absorption spectrometer is simple and is shown schematically in Figure 2.3. The most important components are a radiation source, which emits the spectrum of the analyte element; an atomizer, such as flame, in which the atoms of the sample to be analyzed are formed; a monochromator for the spectral dispersion of the radiation with an exist slit for selection of the resonance line; a detector permitting measurement of radiation intensity, followed by an amplifier and a readout device that presents a reading.

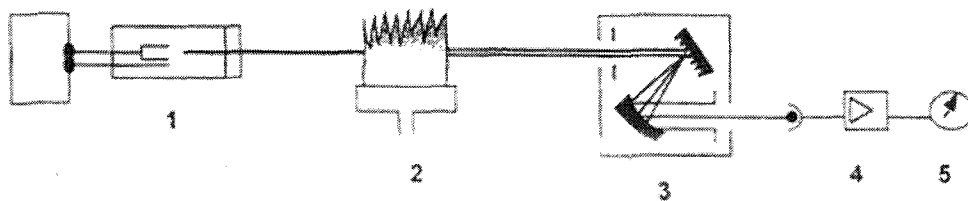


**Figure 2.3.** Schematic representation of an atomic absorption spectrometer. 1 Radiation source, 2 Flame, 3 Monochromator, 4 Detector, 5 Electrical measuring system with readout device.

#### **2.4.1.1. Radiation sources**

Since atoms are only able to absorb radiation within a very narrow frequency interval, certain demands must be placed upon the radiation source. Most common source for atomic absorption measurement is the hollow cathode lamp. A hollow cathode lamp consist of a glass cylinder filled with an inert gas (argon or neon) under a pressure of several hundred Pascal (a few Torr) into which an anode and a cathode have been fused. The cathode is generally in the form of a hollow cylinder and is either made of the analyte metal or filled with it. The anode is in the form of a thick wire, usually of tungsten or nickel.

The efficiency of the hallow cathode lamp depends upon its geometry and the operating potential. High potentials, and thus high currents, lead to greater intensities. This advantage is offset somewhat by an increase in Doppler broadening of the emission lines. Furthermore, the greater currents result in an increase in the number of unexcited atoms in the cloud; the unexcited atoms, in turn, are capable of absorbing the radiation emitted by the excited ones. The self-absorption leads to lowered intensities, particularly at the center of the emission band.

#### **2.4.1.2. Atomizers**

The emission spectrum of the analyte element emitted from the radiation source is passed through an 'absorption cell' in which a portion of the incident radiation is absorbed by atoms produced by thermal dissociation, for example. Accordingly, the most important function of this absorption of this absorption cell is to produce analyte atoms in the ground state from the ions or molecules present in the sample. This is without doubt the most difficult and critical process within the whole atomic absorption procedure. The success or failure of a determination is virtually dependent upon the effectiveness of the atomization; the sensitivity of the determination is directly proportional to the degree of atomization of the analyte element in the sample.

In flame atomization, a solution of the sample is sprayed into a flame by means of a nebulizer, which converts the sample solution into a mist made up of tiny liquid droplets. A complex set of interconnected processes then occurs; these processes ultimately lead to a mixture of analyte atoms, analyte ions, sample molecules, oxide molecules of the analyte, and undoubtedly a variety of other atomic and molecular species formed by reactions among the fuel, the oxidant, and the sample. With so many complex processes occurring, it is not surprising that the atomization is the most critical step in flame spectroscopy and the one that limits the precision of such methods.

Table 2.1 lists the common fuels and antioxidants employed in flame spectroscopy and the appropriate range of temperatures realized with each of these mixtures. The burning velocities listed in the fourth column of the table are of considerable importance, because flames are stable in certain ranges of flow rates only. If the flow rate does not exceed the burning velocity, the flame propagates itself back into the burner, giving flashback. As the flow rate increases, the flame rises until it reaches a point above the burner where the flow velocity and the burning velocity are equal. This region is where the flame is stable. At higher flow rates, the flame rises and eventually reaches a point where it blows off the burner. Clearly, the flow rate of the fuel/oxidant mixture is an important variable that has to be closely controlled.

**Table 2.1.** Properties of flames

<b>Fuel</b>	<b>Oxidant</b>	<b>Temperatures, °C</b>	<b>Burning velocity cm s<sup>-1</sup></b>
Natural gas	Air	1700-1900	39-43
Natural gas	Oxygen	2700-2900	379-390
Hydrogen	Air	2000-2100	300-440
Hydrogen	Oxygen	2550-2700	900-1400
Acetylene	Air	2100-2400	158-266
Acetylene	Oxygen	3050-3150	1100-2480
Acetylene	Nitrous oxide	2600-2800	285

Electrothermal atomizers generally provide enhanced sensitivity because the entire sample is atomized in a short period, and the average residence time of the atoms in the optical path is a second or more.

In electrothermal atomizers, a few microliters of sample are first evaporated at low temperature and then ashed at a somewhat higher temperature in an electrically heated graphite tube or cup. After ashing, the current is rapidly increased to several hundred amperes, which causes the temperature to soar to perhaps 2000°C to 3000°C; atomization of the sample occurs in a period of a few milliseconds to seconds.

#### **2.4.1.3. Optics**

The spectral range of interest for atomic absorption spectrometry begins in the near infrared at 852.1 nm, the wavelength of cesium, and reaches down into the vacuum UV below 200 nm. Atomic absorption spectrometry therefore covers much the same wave length range that is of interest for atomic emission spectrometry or UV/VIS spectrometry. In principle it should then be possible to employ proven monochromators in atomic absorption. However, it has been shown that the requirements in AAS with respect to resolution and dispersion of the monochromator are different from those of other techniques. One of the greatest advantages of atomic absorption spectrometry, namely its specificity is based on the use of element-specific radiation sources that emit the spectrum of the analyte element in the form of very narrow spectral lines. While the quality of an instrument in other spectrometric techniques frequently depends on the resolution of the monochromator or on its spectral bandpass, the range of radiation that passes through the exit slit, these factors are not of primary importance in AAS. The monochromator in an atomic absorption spectrometer has the sole task of separating the resonance line of the analyte element from other emission lines of the source. Prisms and gratings serve to disperse the radiation into individual wavelengths.

#### **2.4.4.4. Detectors**

Photomultipliers are mainly used in atomic absorption spectrometry to convert optical radiation into an electrical signal. They consist of a vacuum photocell with an anode, a radiation sensitive electrode (photocathode), and a number of emission cathodes (dynodes), which have increasing positive potential with respect to the photocathode.

#### **2.4.2. Interferences in atomic absorption spectrometry**

The presence of other constituents accompanying the analyte element in the sample can lead to interferences, which can cause systematic errors in the determination. The influence of the atomizing medium, such as the flame, graphite material, or quartz cell, or of the solvent is not regarded as interference since sample and reference solutions are affected to equal degrees. An interference will cause an error in the analytical result only if the interference is not adequately accounted for in the evaluation procedure. In spectrochemical analysis, interferences are generally divided into two classes: spectral interferences and non-spectral interferences.

##### **2.4.2.1. Spectral interferences**

Spectral interferences are caused by the incomplete isolation of the radiation absorbed by the analyte element from other radiation or radiation absorption due to, or affected by, the interferent. Spectral interferences can arise from:

- ✓ Absorption of the source radiation on non-volatilized particles from concomitants.
- ✓ The indirect influence of concomitants on the blank background absorption or scattering of the atomizer.
- ✓ The indirect influence of concomitants on the blank background absorption or scattering of the atomizer.
- ✓ By sorption of foreign radiation if, in addition to the analytical line, the source emits further radiation within the spectral bandpass of the monochromator. This effect is observed particularly when a continuum source is used.

Several methods have been developed for correcting for interferences;

- ❖ The two line correction method,
- ❖ The continuous-source correction method,
- ❖ Background correction based on the Zeeman effect,
- ❖ Background correction based on source self-reversal.

The continuous source correction method, for background corrections that is widely used. Here a deuterium lamp provides a source of continuous radiation throughout the ultraviolet region. The configuration of the chopper is such that radiation from the continuous source and the hollow cathode lamp are passed through the atomizer. The absorbance of the deuterium radiation is then subtracted from that of the analyte beam. The slit width is kept sufficiently wide so that the fraction of the continuous source that is absorbed by the atoms of the sample is negligible. Therefore, the attenuation of its power during passage through the atomized sample reflects only the broad band absorption or scattering by the sample matrix components. A background correction is thus achieved.

#### **2.4.2.2. Non-spectral interferences**

Non-spectral or chemical interferences result from various chemical process occurring during atomization that the analyte signal is affected directly. Perhaps the most common type of interference is by anion, which form compounds of low volatility with the analyte and thus reduce the rate at which it is atomized. Interference due to formation of species of low volatility can often be eliminated or moderated but use of higher temperatures. Alternatively, releasing agent, which are cations that are react preferentially with the interference and prevents its interaction with the analyte, can be employed. Protective agents prevent interference by forming stable but volatile species with the analyte. An ionization buffer is added to suppress ionization. By adding an easily ionized element, such as cesium or potassium, the concentration of the free electrons in the absorption volume is increased substantially, thereby suppressing and stabilizing ionization of the analyte.

## 2.5. Iron

Iron is the fourth most abundant element in the earth's crust, it is present in a variety of rock and soil minerals both as iron(II) and iron(III) (Taylor et al., 1985). Both of them are important in the biosphere, serving as an active center of a wide range of proteins such as oxidases, reductases and dehydrases (Cotton et al., 1988). These oxidation states are involved in the formation of soluble inorganic and organic complexes, colloids and particulate phases. The  $\text{Fe}^{3+}$  oxidation state predominates in oxygenated waters and is highly insoluble through the formation of oxyhydroxides.  $\text{Fe}^{2+}$  is thermodynamically unstable in oxygenated seawater and its rapidly oxidized to  $\text{Fe}^{3+}$ . Several workers have detected  $\text{Fe}^{2+}$  in surface waters and upwelling regions, reporting contributions of as much as 50% of total dissolved iron (Hong et al., 1986; Gledhill et al., 1995). Potential sources of  $\text{Fe}^{2+}$  are photoreduction of  $\text{Fe}^{3+}$  in surface waters (Miller et al., 1995), atmospheric deposition (Zhuang et al., 1992), and diffusion from sediments (Hong et al., 1986). Thermodynamically speciation calculations indicate that a major fraction (76%) of the total Fe(II) exists in a free hydrated form ( $\text{Fe}^{2+}$ ), with the remaining fraction as  $\text{FeCO}_3$  (Millero et al., 1995). However, recent studies have indicated the possibility of complexation of  $\text{Fe}^{2+}$  by organic ligands, thereby maintaining  $\text{Fe}^{2+}$  concentrations in seawater by decreasing the rate of oxidation to  $\text{Fe}^{3+}$  (Rue et al., 1997). The observed concentrations of total dissolved iron in natural water systems vary from  $0.2 \text{ nmol L}^{-1}$  in mid-ocean surface water (Martin et al., 1989) up to  $400 \text{ } \mu\text{mol L}^{-1}$  in polluted urban clouds (Munger et al., 1983).

Only a small fraction of dissolved  $\text{Fe}^{3+}$  occurs in a free hydrated ( $\text{Fe}^{3+}$ ) or inorganically complexed form, and 80-99% is strongly complexed by organic ligands (Gledhill et al., 1995; Nolting et al., 1998), possibly produced by iron limited phytoplankton (Rue et al, 1997) or bacteria (Granger et al., 1999).

There are four types of Fe exposure in animals and humans according to the present level of knowledge.



The first type is a Fe intake by domestic animals and game via feed-stuffs and fodder, which considerably exceeds the requirement. This reduces feed consumption and influences various metabolic processes without acute “acute symptoms”. The second type is acute poisoning. The third type is a specific form of chronic Fe over-load, hereditary hemochromatosis. The fourth type is the chronic Fe overload resulting from the multiple blood transfusions for chronic anaemia.

The first real assessment of the dangers of acute Fe intoxication was the report of Forbes (1947), in which he described the death of two children after the ingestion of a mixture containing ferrous sulphates. Death may occur from ingestion of as little as 2 to 4 g ferrous sulphate by small children. The symptoms of Fe poisoning are summarized in Table 2.2.

High Fe offers reduce the Cu and Mn content of the liver significantly (Anke et al., 1975; Grun et al., 1978; Gruden, 1977; Fransson et al., 1985).

In humans Fe poisoning or Fe exposure can result from carelessness when dealing with Fe preparations, from hereditary hemochromatosis and multiple blood transfusions (Forth et al., 1984).



**Table 2.2.** The biological importance of iron exposure.

Fe poisoning:	Forbes (1947)
Fe exposure animals:	500 mg/kg ration dry matter reduce the feed consumption and growth in various species of animals, decrease the Mn and Cu content of the liver, reproduction disorder;
Humans, acute Fe poisoning:	vomiting, diarrhoea, coma; bleedings in the gastro-intestinal tract 6 to 24 h, fever, leucocytosis, metabolic acidosis blood clotting disorders, liver and kidney damage, cicatrices in the gastrointestinal Tract, application of desferrioscamin;
Hereditary hemo-chromatosis:	Fe overload with associated tissue damage
transfusional Fe Overload:	$\beta$ -thalassemia, some sickle cell disease, aplastic anaemia, myelofibrosis, desferox-Amine therapy;
Species specificity:	no experimental data;
antagonists:	Mn, Cu, Zn
Fe requirement:	40-75 mg/kg ration dry matter in domestic animals;
Fe intake of humans;	Men, adolescents 12 mg/day, women 15 mg/day Babies 0.8 mg/kg bodyweight, 8-22 mg/day, as a rule 10 to 20 day;
Indicator organs:	hemoglobin, hematocrit, spleen, liver.

## 2.6. Molecular Imprinting

In molecular imprinting (MIP), the target molecule (or a derivative thereof) acts as the template around in which interacting and cross-linking monomers are arranged and co-polymerized to form a cast-like shell (Figure 2.4.). Initially, the monomers form a complex with the template through covalent and non-covalent interactions.

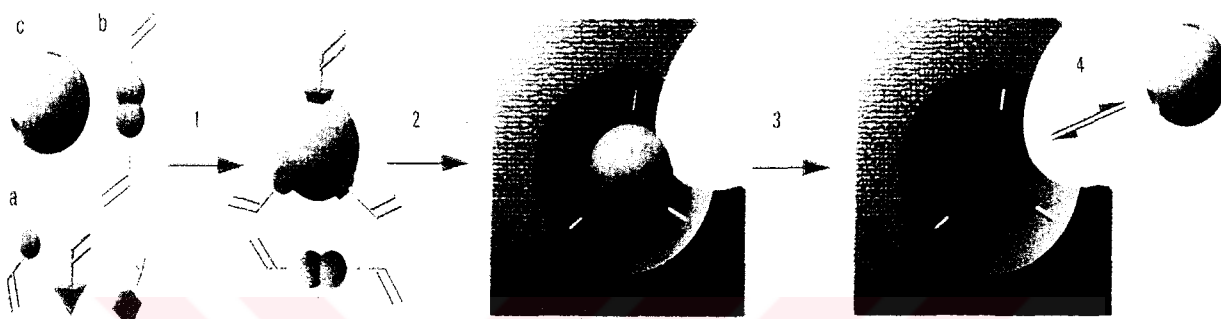


**Figure 2.4.** Creating a molecular imprint in a synthetic polymer. (a) Functional monomers, (b) a cross linker, and (c) a template molecule are mixed together. (1) The functional monomers copolymerize with the cross-linker. (3) As polymerization proceeds, an insoluble, highly cross-linked polymeric network is formed around the template. (4) removing the template liberates complementary binding sites that can reaccommodate the template in a highly selective manner.

After polymerization, the template is removed, and binding sites are exposed that are complementary to the template in size, shape, and position of the functional groups. In essence, a molecular “memory” is imprinted on the polymer, which is now capable of selectively rebinding the template (Katz and Davis, 2000).

### 2.6.1. Imprinting at surfaces

Imprinted materials with binding sites situated at or close to the surface of the imprinting matrix have many advantages - the sites are more accessible, mass transfer is faster, the binding kinetics may be faster, and the target molecules conjugated with bulky labels can still bind. Unfortunately, these materials are not

universally used because their preparation is less straight forward than that of bulk polymers, and they require specially adapted protocols. Withcombe and co-workers have developed a technique based on emulsion polymerization in which small beads are created in oil-in-water biphasic system stabilized by a surfactant.

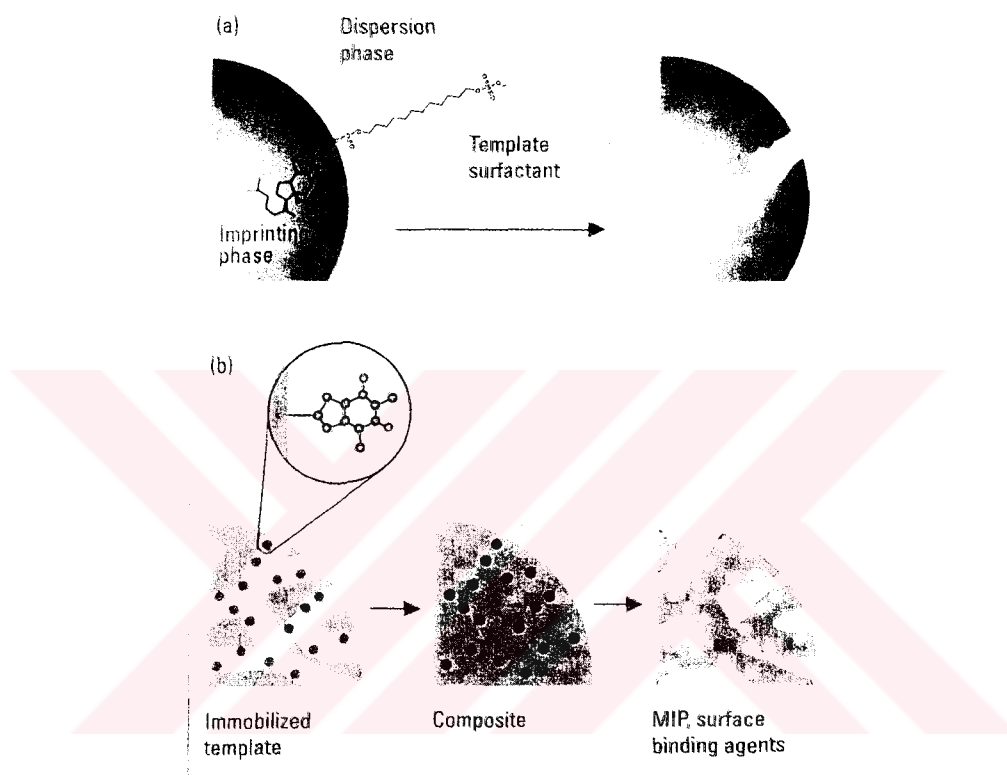


**Figure 2.5.** Imprinting at surfaces.

(a) Synthesis of cholesterol-imprinted nanospheres by emulsion polymerization using a template surfactant. (b) Molecular imprinting of a theophylline template immobilized onto a solid support.

The imprint molecule, in this case cholesterol, is part of the surfactant pyrdinium 12-(cholesteryloxycarbonyloxy)dodecane sulfate (Perez et al., 2001). As a result, all binding sites are situated at the particle surface (Figure 2.5a.), which was demonstrated by flocculation experiments using polyethylene glycol-bis-cholesterol.

Also, another protocol for creating surface binding sites is introduced. The imprinting molecule is immobilized onto a solid support such as porous silica beads prior to polymerization (Yilmaz et al., 2000). The pores are then filled with the monomer mixture, and the polymerization is initiated. The silica is removed by chemical dissolution, leaving behind a porous polymeric structure, which is the negative image of the original bead. The binding sites are now all situated at the surface of the polymer and are uniformly oriented (Figure 2. 5b.)

MIPs can be synthesized at an electrode surface by electropolymerization (Panasyuk et al., 1999) or at a nonconducting surface by chemical grafting (Piletsky et al., 2000), or by using polymerization initiators chemically bound (Sulitzky et al., 2002) or physically adsorbed (Panasyuk-Delaney et al., 2001) to the surface. These methods yield binding sites contained in the bulk of the MIP layer, but if a highly porous starting material is used and if the grafted layer is relatively thin, mass transfer is facilitated. For example, Ulbricht and co-workers have photografted a MIP layer that is 10 nm thick in the dry state onto a polypropylene membrane (Piletsky et al., 2000). Sellergren's group synthesized MIP layers at the pore surface of porous silica particles and was able to control the thickness in the nanometer range (Sulitzky et al., 2002).

Wulff (Wulff, 1995) produced MIPs for carbohydrates, amino acids and their derivatives by covalent molecular imprinting. Haupt and Mosbach (Haupt and Mosbach, 2000) developed the so called non-covalent approach for the resolution of optical enantiomers, biomolecules etc. Furusaki and coworkers (Uezu, 1999) developed a novel molecular imprinting technique called surface template polymerization in which the coordinated structure is eventually imprinted on polymer surface, not in the polymer matrix. These MIP materials are used in thin layer chromatography, capillary electrochromatography, sensors and membrane-based separations.

Ion imprinting polymer (IIP) materials by copolymerization chloroacrylic acid and ethylene glycol dimethacrylate with uranyl ion as imprint ion, which after removal the template, selectively extracts uranium from dilute aqueous solutions over a range of +2, +3 and +4 competitor metal ions (Saunders et al., 2000). Murray co-workers (Bae et al., 1999) have described the synthesis of ion imprinting resin by copolymerizing uranium-vinyl benzoate complex, styrene and divinyl benzene using 2,2'-azo bis isobutyronitrile as initiator for the preconcentration of uranyl ion from the dilute solutions. Lemaire and co-workers (Vigneau et al., 2001), (Vigneau et al., 2002) have developed ion imprinted resins based on EDTA and DTPA derivatives for the selective separation of Gd from La, Nd, Eu and Lu ions.

## **2.6.2. Applications**

### **2.6.2.1. Separations**

The application in which MIPs are closest to commercialization is sample preparation for biomedical, environmental, and food analysis (Lanza and Sellergen, 2001), (Andersson, 2001). A Swedish start-up company is already producing a solid-phase extraction (SPE) material for clenbuterol. For SPE, MIPs seem to be just perfect; compared with immunoextraction sorbents, MIPs are relatively stable, have a higher adsorption capacity, can easily be obtained for small analytes, and could be cheaper to produce.

In the context of SPE, however, the MIP fabrication procedure poses an intrinsic problem. After synthesis, a few percent of the template molecules are imprisoned in the highly crosslinked polymer matrix and can not easily washed out. Some of these remaining template molecules will inevitably leach out and falsify the results. Some researchers have had success with washing procedures to completely remove the template (Ellwanger et al., 2001). Others have used a "dummy template" -the imprint is created not with the target analyte itself, but with a structurally related molecule. The polymer can still bind the target analyte, but the leaching template does not coelute with the analyte during chromatographic analysis.

### **2.6.2.2. Sensors**

Because of their superior stability, MIPs are attractive recognition elements in sensors, and many different transducers have been used in combination with MIPs (Haupt and Mosbach, 2000). In particular, the quartz crystal microbalance, an acoustic transducer, has become very popular, probably because of its comparatively low price, robustness, and ease of use.

An elegant way to generate the sensor response is to incorporate reporter groups into the polymer, which increases sensitivity and S/N. For example, Takeuchi and co-workers used a polymerizable derivative of a fluorescent metalloporphyrin as one of the functional monomers (Matsui et al., 2000). Binding of the analyte 9-ethyladenine to the MIP resulted in quenching the polymer's fluorescence.

### **2.6.2.3. Drug development and screening**

A few preliminary reports with small libraries have demonstrated the feasibility of using MIPs as artificial receptors to screen combinatorial libraries (Ramstrom et al., 1998), (Ye et al., 2001). MIPs might work well for the initial screening of large libraries because they are well adapted to high-throughput methods. Haupt reported a high-performance, MIP-based assay using a chemiluminescence-imaging format as a screening tool (Surugiu et al., 2001). The analyte is added to microtiter plates coated with MIP microspheres along with a small amount of enzyme (peroxidase)-labeled analyte the incubated until equilibrium reached. After unbound conjugate is washed away, the amount of polymer-bound analyte-peroxidase conjugate is detected by using a chemiluminescent substrate. Light emission is quantified with a CCD camera-based imaging system, which allows for the simultaneous measurement of a large number of samples. To further speed up to screening, a homogeneous assay may be used. A reporter group is introduced into a quantifiable signal. The bound fraction of the labelled analyte is quantified without separating it from the free fraction described above.

Ye and co-workers combined MIPs with proximity scintillation (Ye and Mosbach, 2001). A scintillation flour is randomly and covalently incorporated into a MIP by copolymerization. When the scintillation flour is irradiated with  $\beta$ -rays, it emits fluorescent light that can be quantified with a photomultiplier tube. They used small MIP microspheres that were stable in suspension for the time required for the measurement.

#### **2.6.2.4. Directed synthesis**

Withcombe and co-workers proposed using MIPs as protecting groups for regioselective synthesis (Alexander et al., 1999). They imprinted a polymer with a steroid with one additional hydroxyl groups. In an acylation reaction of a steroid with one additional hydroxyl, the MIP then protected the two original ones and directed the derivatization to the third one. Recently, Mosbach and co-workers created a technique in which the binding sites of a MIP are used as molecular-scale reaction vessels to direct the synthesis of new enzyme inhibitors (Mosbach et al., 2001), (Yu et al., 2002). They synthesized a polymer imprinted with a known inhibitor for the enzyme kallikrein. Different inhibitor building blocks were then allowed to assemble and interconnect in the imprinted site, leading to combinatorial library new enzyme inhibitors (Figure 2.6.). They were even able to use the enzyme itself to direct the inhibitor synthesis, which yielded similar results (Yu et al., 2002). This method is somewhat related to click chemistry (Lewis et al., 2002) and dynamic combinatorial chemistry (Lehn, 1999). It might allow new molecules with biological activity to be found for target biological receptors that have not been well studied. The use of a MIP, however, opens a new dimension –the enzyme or receptors does not need to be isolated or even known; new effectors can be identified using a MIP as a synthetic receptors.

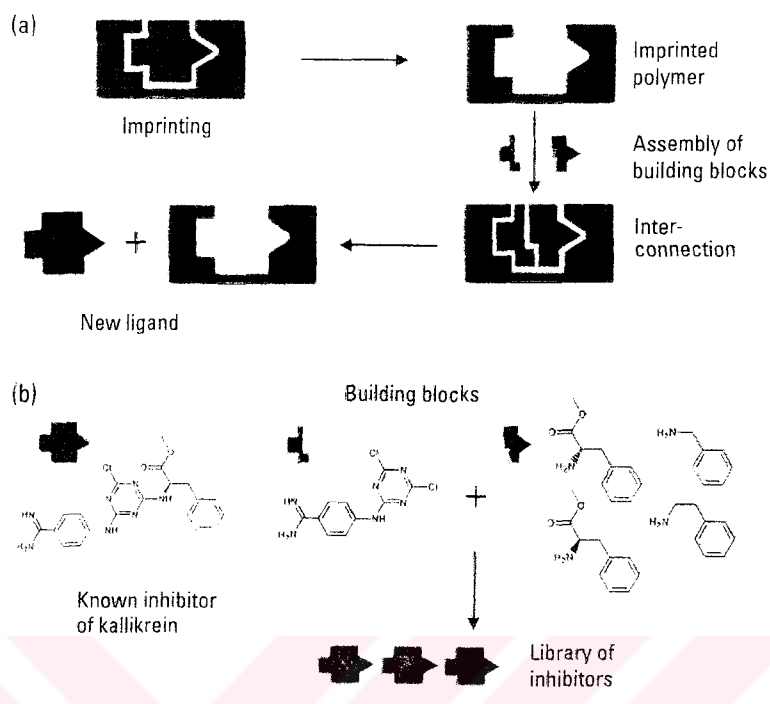


**Figure 2.6.** (a) Synthesis of a new ligand in the binding site of a MIP. The polymer is imprinted with a known ligand (substrate, inhibitor, etc.). The binding sites are then used as molecular-scale reaction vessels for the synthesis of new ligands by assembling building blocks from a combinatorial library. (b) Synthesis of inhibitors of kallikrein.

Many academic research groups have shown that, in principle, MIPs can be used in plethora of applications, but the time is long past where the proof of principle was sufficient to raise interest for investment. Companies need to investigate MIP target selectivity and compatibility with the environmental in which they are to be used, including biological fluids and tissues. The integration of molecular imprinting into existing industrial fabrication processes, yields, cost and the competitiveness of MIPs with existing materials must also be examined. The recent appearance of several startup companies working in molecular imprinting field is a very good sign.



### **3. EXPERIMENTAL**

#### **3.1. Materials**

Cysteine and methacryloylchloride were supplied by Sigma (St. Louis, MO, USA) and used as received. 2-Hydroxyethylmethacrylate (HEMA) and ethyleneglycol dimethacrylate (EGDMA) were obtained from Fluka (Buchs, Switzerland), distilled under reduced pressure in the presence of hydroquinone inhibitor and stored at 4°C until use. Benzoyl peroxide (BPO) was also obtained from Fluka (Switzerland). Poly(vinylalcohol) (PVAL;  $M_w$ : 100.000, 98% hydrolyzed) was supplied from Aldrich Chemical (USA). All other chemicals were of reagent grade and purchased from Merck (Darmstadt, Germany). All water used in the experiments was purified by using a Barnstead (Dubuque, IA, USA) RO pure LP reverse osmosis unit with a high flow cellulose acetate membrane (Barnstead D2731) followed by a Barnstead D3804 NANO pure organic/colloid removal and ion exchange packed bed system. The purified water (deionized water) has a specific conductivity of 18 M $\Omega$ .

#### **3.2. Preparation of Polymeric Beads**

##### **3.2.1. Synthesis of 2-methacryloylamidocysteine**

The following experimental procedure (Denizli et al., 2003) was applied for the synthesis of 2-methacryloyl-amidocysteine (MAC) monomer: 5.0 g of cysteine and 0.2 g NaNO<sub>2</sub> were dissolved in 30 mL of K<sub>2</sub>CO<sub>3</sub> aqueous solution (5% v/v). This solution was cooled down to 0 °C. 4.0 mL of methacryloylchloride was poured slowly into this solution under nitrogen atmosphere and then this solution was stirred magnetically at room temperature for 2 h. At the end of this period, the pH of this solution was adjusted to 7.0 and then reaction mixture was extracted with ethylacetate. Aqueous phase was evaporated in a rotary evaporator. The residue was crystallized in ethanol and ethylacetate.

### 3.2.2. Preparation of Fe<sup>3+</sup>-imprinted poly(HEMA-co-MAC) beads

In the first part, MAC-Fe<sup>3+</sup> complex was prepared. In order to prepare MAC-Fe<sup>3+</sup> complex, solid 2-methacryloylamidocysteine (MAC) (0.378 g, 2.0 mmol) was added slowly into 15 mL of ethanol and then treated with Fe(NO<sub>3</sub>)<sub>3</sub>·9H<sub>2</sub>O (0.404 g, 1.0 mmol) at room temperature with conditions stirring for 24 h. Then the formed metal-comonomer complex was filtered, then washed with 99% ethanol, and dried in a vacuum oven.

2-hydroxyethylmethacrylate (HEMA) and MAC were copolymerized in suspension by using benzoyl peroxide (BPO) and poly(vinyl alcohol) as the initiator and the stabilizer, respectively. Toluene and EGDMA was included in the recipe as the diluent (as a pore former) and crosslinker, respectively. Table 3.1. gives the polymerization recipe and experimental conditions to obtain Fe<sup>3+</sup>-imprinted poly(HEMA-co-MAC) beads in the size range of 150-200 μm (in swollen form).

**Table 3.1.** Recipe and polymerization conditions for the preparation of Fe<sup>3+</sup>-imprinted poly(HEMA-co-MAC) beads with a swelling ratio of 72 % and in the size range of 150-200 μm.

---

#### Aqueous Dispersion Phase

Distilled water: 50 mL

PVAL : 0.2 g

#### Organic Phase

MAC-Fe<sup>3+</sup>: 500 mg

HEMA : 4.0 mL

EGDMA : 8.0 mL

Toluene : 12 mL

BPO : 0.1 g

#### Polymerization conditions

Reactor volume : 100mL

Stirring range : 600 rpm

Temperature & Time: First at 65°C for 4h, and then at 90° C for 2 h.

---

### 3.2.3. Removal of the template (Fe<sup>3+</sup> ions)

In order to remove unreacted monomers and other ingredients the beads were extensively washed with methanol/water solution (60/40) for 24 h at room temperature. After cleaning procedure, the template was removed from the polymer beads using 0.1 M HCl. The imprinted beads were added into the 0.1 M HCl solution for 48 hours at room temperature. The template free polymers were cleaned with 0.1 M HNO<sub>3</sub> in a magnetic stirrer for 3 hours.

## 3.3. Characterization of Polymeric Beads

### 3.3.1. Surface area measurements

The specific surface area of the p(HEMA-co-MAC) beads was determined with a BET apparatus. The average size and size distribution of the p(HEMA-co-MAC) beads were determined by screen analysis performed by using Tyler Standart Sieves.

### 3.3.2. Swelling test

Swelling ratio of the p(HEMA-co-MAC) beads was determined in distilled water. The experiment was conducted as follows: initially dry beads sample were carefully weighed before being placed in a 50 mL vial containing distilled water. The vial was put into an isothermal water bath with a fixed temperature (25±0.5 °C) for 2 h. The bead sample was taken out from the water, wiped using a filter paper, and weighed. The ratio of dry and wet samples was recorded. The water content of the p(HEMA-co-MAC) and the Fe<sup>3+</sup>-imprinted p(HEMA-co-MAC) beads were calculated by using the following expression:

$$\text{Water uptake ratio \%} = [(W_s - W_o) / W_o] \times 100 \quad (3.1)$$

Where  $W_o$  and  $W_s$  are the weighs of beads before and after uptake of water, respectively.

### **3.3.3. Elemental Analysis**

Elemental nitrogen analysis of the p(HEMA-co-MAC) beads was carried out at the TUBITAK Technical Services Laboratory (Ankara, Turkey) revealing that the incorporated MAC density was  $3.9 \text{ mmol g}^{-1}$ .

### **3.3.4. FTIR Studies**

FTIR spectra of the p(HEMA-co-MAC) beads was obtained by using a FTIR spectrophotometer (FTIR 8000 Series, Shimadzu, Japan). The dry beads (about 0.1 g) was thoroughly mixed with KBr (0.1 g, IR Grade, Merck, Germany), and pressed into a pellet and the FTIR spectrum was then recorded.

## **3.4. Fe<sup>3+</sup> Ions Adsorption/Desorption Studies in Batch System**

### **3.4.1. Reagents and apparatus**

Adsorption of Fe<sup>3+</sup> and Fe<sup>2+</sup> ions on the Fe<sup>3+</sup>-imprinted p(HEMA-co-MAC) beads were studied in batch experiments. All reagents were of analytical reagent grade unless otherwise stated. 18 MΩ distilled de-ionized (DDI) water purified with a Barnstead (Dubuque, IA, USA) was used for the preparation of solutions. Laboratory glassware was kept overnight in a 5% nitric acid solution. Before use the glassware was rinsed with deionised water and dried in a dust-free environment. Stock solutions of 1000 mg L<sup>-1</sup> Fe(III) and Fe(II) were prepared by dissolving iron nitrate (Fe(NO<sub>3</sub>)<sub>3</sub>·9H<sub>2</sub>O) (Merck, Darmstadt, Germany) and ferrous chloride (FeCl<sub>2</sub>·4H<sub>2</sub>O) (BDH, Poole, England) respectively. Standard iron solutions of lower concentration were prepared daily by dilution of the stock solutions. Accumet, model 15 (Fischer Scientific) pH-meter was used for adjusting the pH values.

Effects of Fe<sup>3+</sup> and Fe<sup>2+</sup> initial concentrations and pH of the medium on the adsorption rate and adsorption capacity were studied. 25 mL of aliquots of aqueous solutions containing different amount of Fe<sup>3+</sup> and Fe<sup>2+</sup> ions in the range of 1-70 mg L<sup>-1</sup> were treated with the polymer beads at different pH in the range of

2-5 (adjusted with HCl-NaOH). 50 mg of Fe<sup>3+</sup>-imprinted p(HEMA-co-MAC) beads were stirred with a iron (III) nitrate and iron (II) chlorine salt solutions at room temperature for 1 h with stirring rate 400 rpm. The concentrations of the Fe ions in the aqueous phase, after the desired treatment periods was measured by using a Perkin-Elmer AAnalyst 800 atomic absorption spectrometer with deuterium background correction equipped with Perkin-Elmer single element hollow cathode lamps was used. A Perkin-Elmer hollow cathode iron lamp was used. The working current/wavelength was 30 mA per 248.3 nm with spectral bandwidth of 0.5 nm. The instrument response was periodically checked with known Fe<sup>3+</sup> and Fe<sup>2+</sup> solution standards. The experiments were performed in replicates of three as well. For each set of data present, standard statistical methods were used to determine the mean values and standard deviations. Confidence intervals of 96% were calculated for each set of samples in order to determine the margin of error. The amount of Fe adsorption per unit mass of the beads was evaluated by using the following expression:

$$Q = [(C_0 - C) \cdot V] / m \quad (3.2)$$

Where, Q is the amount of Fe ions adsorbed onto unit mass of beads ( $\mu\text{mol g}^{-1}$ ); C<sub>0</sub> and C are the concentrations of the Fe ions in the initial solution and in the aqueous phase after treatment for certain period of time, respectively ( $\mu\text{mol L}^{-1}$ ); V is the volume of the plasma (L); and m is the mass of the beads used (g).

#### 3.4.2. Selectivity experiments

In order to show Fe<sup>3+</sup> specificity of the Fe<sup>3+</sup>-imprinted p(HEMA-co-MAC) beads, Fe<sup>2+</sup> was chosen its different oxidation state and its toxic behaviour in this state Zn<sup>2+</sup> and Cu<sup>2+</sup> was chosen which they have toxic behaviour, and Cr<sup>3+</sup> was chosen which is same oxidation state as Fe<sup>3+</sup>.

In selectivity experiments, competitive adsorption of  $\text{Fe}^{3+}/\text{Fe}^{2+}$ ,  $\text{Fe}^{3+}/\text{Cr}^{3+}$ ,  $\text{Fe}^{3+}/\text{Cu}^{2+}$ , and  $\text{Fe}^{3+}/\text{Zn}^{2+}$  from their binary solutions and  $\text{Fe}^{3+}$ ,  $\text{Cr}^{3+}$ ,  $\text{Cu}^{2+}$  and  $\text{Zn}^{2+}$  from their mixture of solutions were investigated. Solutions containing  $25 \text{ mg L}^{-1}$  of metal ions were treated with 50 mg of  $\text{Fe}^{3+}$ -imprinted p(HEMA-co-MAC) beads for 1 h at pH 3, in the flasks stirred magnetically at 400 rpm. After adsorption equilibrium, the concentration of the metal ions in the remaining solution was measured by a FAAS system. A Shimadzu M 1240 UV-VIS spectrophotometer was used for the determination of  $\text{Fe}^{2+}$  in the mixture of  $\text{Fe}^{3+}/\text{Fe}^{2+}$ . Spectrophotometric detection was performed at a wavelength of 510 nm (Vogel, 1986)

The distribution coefficient ( $K_d$ ) gives the ratio of the amount of metal ion adsorbed by 1 g of the adsorbent to the amount of metal ion remained in 1 mL of the solution and distribution ratio ( $k$ ) indicates the strength of metal-binding by adsorbent.

Distribution and selectivity coefficients of  $\text{Fe}^{2+}$ ,  $\text{Cr}^{3+}$ ,  $\text{Cu}^{2+}$  and  $\text{Zn}^{2+}$  with respect to  $\text{Fe}^{3+}$  were calculated as explained by the following equation.

$$K_d = [(C_i - C_f)/C_f] \times V/m \quad (3.3)$$

Where,  $K_d$  is the distribution coefficient;  $C_i$  and  $C_f$  represent the initial and final solution concentrations, respectively.  $V$  is the volume of solution used for the extraction and  $m$  is the weight of polymer used for extraction. The selectivity coefficient  $k$  for the binding of a specific metal ion in the presence of competitor species can be obtained from equilibrium binding data according to:

$$k = K_{\text{template metal}} / K_{\text{interferent metal}} \quad (3.4)$$

(Dai et al., 1999)

### 3.4.3. Effect of interfering ions

The effect of interfering ions has also been studied. Sample solutions containing 5 mg L<sup>-1</sup> of Fe<sup>3+</sup> ions and various amounts of Na<sup>+</sup>, Mg<sup>2+</sup> and Ca<sup>2+</sup> ions as interferants were examined by the general procedure. The chloride, nitrate, carbonate ions are found to be present in natural water and have the capability to complex with many metal ions. Consequently they may reduce the adsorption of metal ions. Thus the effect of NaCl, KCl, Mg(CO<sub>3</sub>)<sub>2</sub> and Ca(NO<sub>3</sub>)<sub>2</sub> on the adsorption of Fe<sup>3+</sup>-imprinted p(HEMA-co-MAC) beads was studied under the optimum conditions.

### 3.5. Desorption and Reuse

The repeated use (i.e. regenerability) of the commercial adsorbent is likely to be a key factor in improving wastewater process economics. Desorption of the adsorbed Fe<sup>3+</sup> ions from the Fe<sup>3+</sup>-imprinted p(HEMA-co-MAC) beads was also studied in batch experimental set-up. Various concentration of HCl, HNO<sub>3</sub>, EDTA and NH<sub>4</sub>SCN were compared for desorption of Fe<sup>3+</sup> ions from the Fe<sup>3+</sup>-imprinted p(HEMA-co-MAH) beads after the adsorption step. In this study, desorption time was found to be 30 minutes at a stirring rate of 400 rpm at room temperature. The final Fe<sup>3+</sup> ions concentration in the desorption medium was measured by atomic absorption spectrometer. The desorption ratio was calculated from the amount of Fe<sup>3+</sup> ions adsorbed on the beads and the final Fe<sup>3+</sup> ions concentration in the desorption medium by the following equation:

$$\text{Desorption Ratio} = \frac{\text{amount of Fe}^{3+} \text{ ions desorbed to the elution medium}}{\text{amount of Fe}^{3+} \text{ ions adsorbed on the beads}} \times 100 \quad (3.5)$$

In order to obtain the reusability of the Fe<sup>3+</sup>-imprinted p(HEMA-co-MAH) beads, adsorption-desorption cycle was repeated five times by using the same imprinted microbeads. The results showed that Fe<sup>3+</sup>-imprinted p(HEMA-co-MAH) beads

could be repeatedly used in  $\text{Fe}^{3+}$  adsorption without any detectable loss in the initial adsorption capacity.

### **3.6. Removal of $\text{Fe}^{3+}$ Ions from Tap-water and Certified Reference Serum**

In order to estimate the accuracy of the procedure, different amounts of the  $\text{Fe}^{3+}$  ions were spiked in tap water. 20 mL sample solution was treated under the general adsorption-desorption procedure.

Removal of  $\text{Fe}^{3+}$  ions from certified reference serum sample with using  $\text{Fe}^{3+}$ -imprinted p(HEMA-co-MAC) beads was also investigated. This reference material is produced from serum collected from thoroughly controlled voluntary blood donors of a Scandinavian blood bank. In order to determine the removal of  $\text{Fe}^{3+}$  ions from the serum,  $\text{Fe}^{3+}$ -imprinted p(HEMA-co-MAC) beads were used for serum samples containing different amounts of  $\text{Fe}^{3+}$  ions.



## 4. RESULTS and DISCUSSION

### 4.1. Properties of Polymer Beads

p(HEMA-co-MAC) beads were spherical in shape with a size range of 150-200  $\mu\text{m}$  in diameter. The specific surface area of the p(HEMA-co-MAC) beads was found to be  $18.9 \text{ m}^2 \text{ g}^{-1}$ . The p(HEMA-co-MAC) beads are crosslinked hydrophilic matrices. The equilibrium swelling ratio of the p(HEMA-co-MAC) beads used in this study, which were prepared with the recipe given Table 3.1., is 72%. Compared with pHEMA (55%), the water uptake ratio of the p(HEMA-co-MAC) beads increases (72%). Several explanations can be offered. First, incorporating MAC actually introduces more hydrophilic functional groups into the polymer chain, which can interact more water molecules into the polymer matrices. Second, reacting MAC with HEMA effectively decreases the molecular weight. Therefore, water molecules penetrate into the polymer chains more easily, resulting in an improvement of polymer water uptake in aqueous solutions. It should be noted that these beads are quite rigid, and strong enough due to cross-linked structure. Therefore, these beads are suitable for packed-bed column applications.

The surface morphology and internal structure of  $\text{Fe}^{3+}$ -imprinted p(HEMA-co-MAC) beads are exemplified by the electron micrographs in Figure 4.1. In Figure 4.1A, the polymeric beads have a spherical form and rough surface due to the pores which formed during the polymerization procedure. The micrograph in Figure 4.1B was taken with broken beads to observe the internal part of the polymeric structure. The presence of the pores within the bead interior is clearly seen in this photograph. It can be concluded that the  $\text{Fe}^{3+}$ -imprinted p(HEMA-co-MAC) beads have a microporous interior surrounded by a reasonably rough surface, in this dry state. The roughness of the bead surface should be considered as a factor providing an increase in the surface area. In addition, these micropores reduce diffusional resistance and facilitate mass transfer because of the high internal surface area.

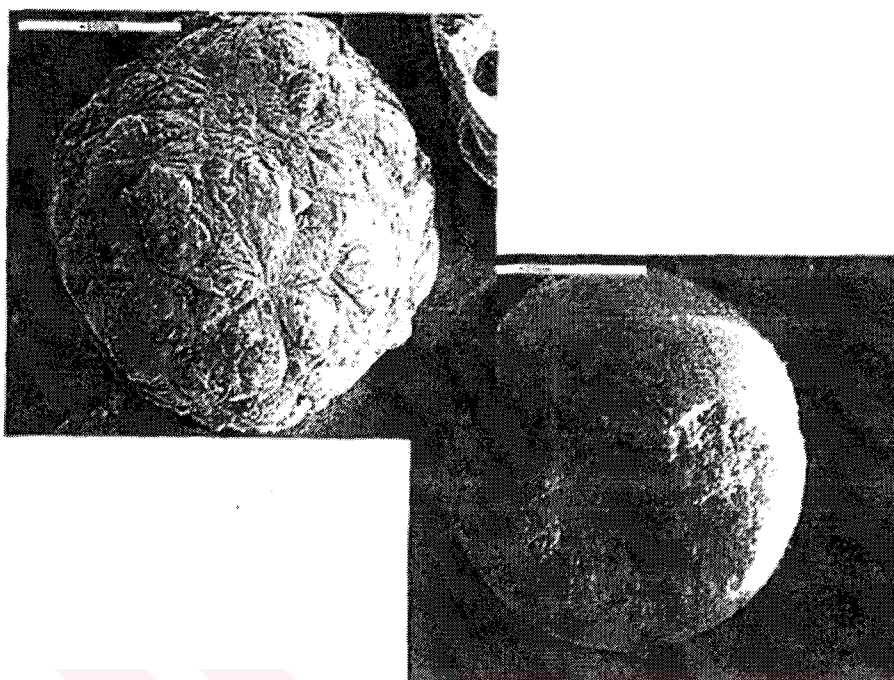


**Figure 4.1.** SEM micographs of  $\text{Fe}^{3+}$ -imprinted p(HEMA-co-MAC) beads (A) surface; (B) cross-section.

To evaluate the degree of MAC incorporation, the elemental analysis of the synthesized p(HEMA-co-MAC) was performed. The incorporation of the MAC was found to be 3.9 mmol MAC  $\text{g}^{-1}$  from the nitrogen stoichiometry.

As mentioned before, MAC was synthesized as the ligand. In the first step, MAC was synthesized from cysteine and methacryloyl chloride. Then, MAC was incorporated into the bulk structure of the pHEMA beads. 2-Methacryloylamidocysteine (MAC) was selected as the comonomer and ion-imprinting ligand for the selective separation of  $\text{Fe}^{3+}$  ions. The molecular formula of synthesized MAC monomer is shown in Figure 4.2. FTIR spectrum of MAC has the characteristic stretching vibration amide I and amide II absorption bands at  $1651\text{ cm}^{-1}$  and  $1558\text{ cm}^{-1}$ , carbonyl band at  $1724\text{ cm}^{-1}$  as shown in Figure 4.3. For the characteristic determination of complex, due to linear coordinate covalent complex formation, the characteristic strong S-H stretching vibration bands at

1130  $\text{cm}^{-1}$  and 970  $\text{cm}^{-1}$  slips to the higher frequency field at 950  $\text{cm}^{-1}$  and 750  $\text{cm}^{-1}$ , as a result of decreasing the electron density of sulfhydryl group of MAC monomer. The Fe-S bands occur at 360 and 348  $\text{cm}^{-1}$  (Silverstein, 1981) (Baruah and Gogoi, 1998) but these bands can not be observed because of the instrumental region is up to 400  $\text{cm}^{-1}$ .

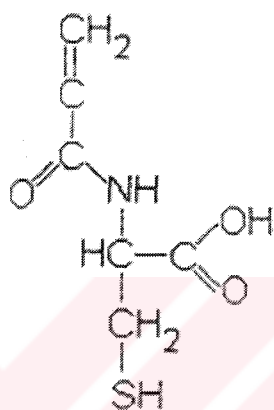


**Figure 4.2.** The molecular formula of MAC monomer.

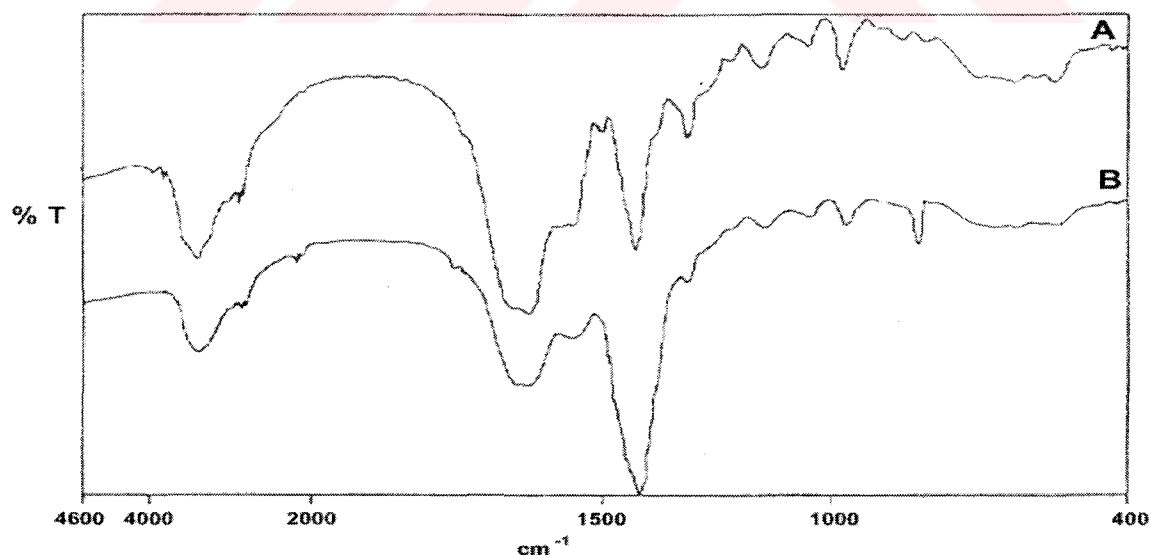


**Figure 4.3.** FTIR spectrum of (A)MAC-Fe<sup>3+</sup> complex-monomer (B) MAC monomer.

FTIR spectra of both MAC and p(HEMA-co-MAC) have the characteristic stretching vibration band of hydrogen bonded alcohol, O-H around  $3649\text{ cm}^{-1}$ . The FTIR spectra of p(HEMA-co-MAC) have characteristic amide I and amide II absorption bands at  $1645$  and  $1456\text{ cm}^{-1}$ , respectively. The molecular formula of p(HEMA-co-MAC) beads is given in Figure 4.4.

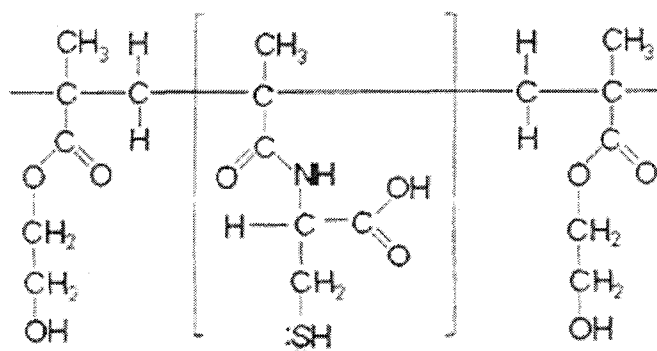


**Figure 4.4.** The molecular formula of p(HEMA-co-MAC) beads.

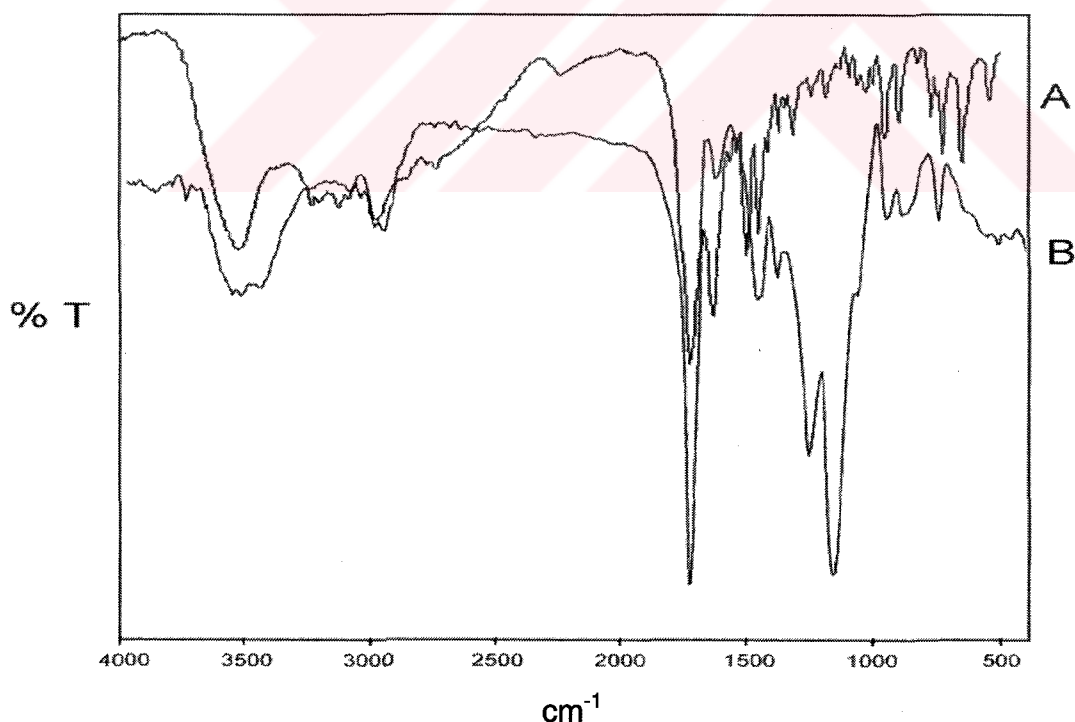


**Figure 4.5.** (A) FTIR spectrum of pHEMA. (B) FTIR spectrum of  $\text{Fe}^{3+}$ -imprinting p(HEMA-co-MAC) beads.

The FTIR spectrum of Fe<sup>3+</sup>-imprinted p(HEMA-co-MAC) beads was shown in Figure 4.5B. Fe<sup>3+</sup>-imprinted p(HEMA-co-MAC) beads has the characteristic stretching vibration band of hydrogen bonded alcohol, O-H, around 3586 cm<sup>-1</sup>, carbonyl at 1645 cm<sup>-1</sup>, amide II absorption bands at 1516 cm<sup>-1</sup>, respectively (Figure 4.5B). On the other hand hydrogen bonded alcohol O-H stretching band intensity of plain pHEMA is higher than that of p(HEMA-co-MAC) beads due to the incorporation of MAC metal-complexing ligand/or comonomer in the polymer structure (Figure 4.5A).

## **4.2. Adsorption of Fe<sup>3+</sup> and Fe<sup>2+</sup> Ions from Aqueous Solutions**

### **4.2.1. Effect of pH**

The metal ion complexation of polymeric ligands and speciation are highly dependent on the equilibrium pH of the medium. In the present study we changed the pH range between 2.0 and 5.0. The effect of pH on the Fe<sup>3+</sup> and Fe<sup>2+</sup> adsorption of this Fe<sup>3+</sup>-imprinted p(HEMA-co-MAC) beads as also shown in Figure 4.6. The Fe<sup>3+</sup>-imprinted p(HEMA-co-MAC) beads exhibited a high affinity in acidic conditions (pH 3.0).

In the literature, 2- Mercaptobenzimidazole loaded on silica gel (MBI-SG) was used for preconcentration and speciation of Fe<sup>2+</sup> and Fe<sup>3+</sup> in water samples. The working pH was pH 2. (Bagheri et al., 2000). In solid phase preconcentration of iron as methylthymol blue complex on naphthene-tetraoctylammonium bromide adsorbent with subsequent flame atomic absorption spectrometer study the results show that maximum recovery of the iron was obtained at pH 3 (Pourreza and Mousavi, 2004). Kara and Alkan used N,N'-bis(2-hydroxy-5-bromobenzyl)1,2 diaminopropane for selective preconcentration, separation and speciation of ferric iron in different samples. They found that the separation factor for the separation of Fe<sup>3+</sup> from other metals 26507 at pH 3.82 (Kara and Alkan, 2001).

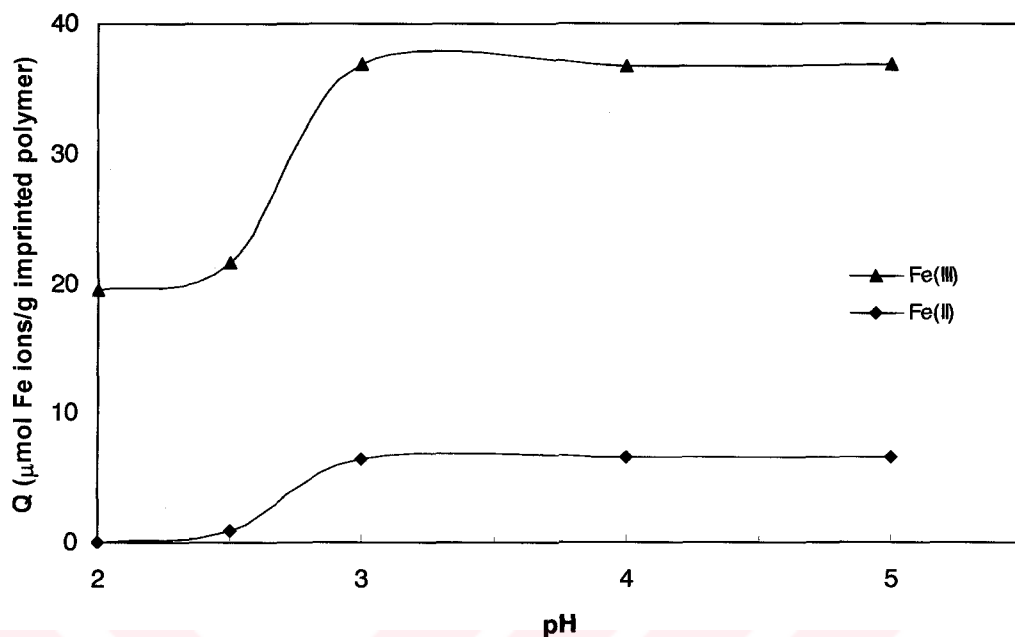


**Figure 4.6.** Effect of pH on  $\text{Fe}^{3+}$  and  $\text{Fe}^{2+}$  adsorption.  $\text{Fe}^{3+}$  and  $\text{Fe}^{2+}$  metal ions initial concentration:  $5 \text{ mg L}^{-1}$ , adsorption time: 30 min., T:  $25^\circ\text{C}$ .

Akerkar and co-workers examined the new chelating resin with a spacer containing  $\alpha$ -nitroso- $\beta$ -naphthol sorption behaviour of  $\text{Fe}^{3+}$  ions. They found that the maximum amount of sorbed  $\text{Fe}^{3+}$  ion at pH 2.5 (Akerkar et al., 1998). Jose and Pillai studied transition metal complexes of polymeric amino ligands derived from triethyleneglycol dimethacrylate crosslinked polyacrylamides. The optimum pH for complexation of  $\text{Fe}^{3+}$  ions was investigated 2.2 (Jose and Pillai, 1996).

#### 4.2.2. Equilibrium adsorption time

Figure 4.7. exemplifies adsorption rates of  $\text{Fe}^{3+}$  and  $\text{Fe}^{2+}$  ions by  $\text{Fe}^{3+}$ -imprinted p(HEMA-co-MAC) beads as a function of time. Note that these batch experiments were performed by using single (not together) solutions of the  $\text{Fe}^{3+}$  and  $\text{Fe}^{2+}$  ions. The slopes of these curves reflect the adsorption rates. As seen here, high adsorption rates are observed at the beginning, and then plateau values (i.e. adsorption equilibrium) are gradually reached within 5-30 min.

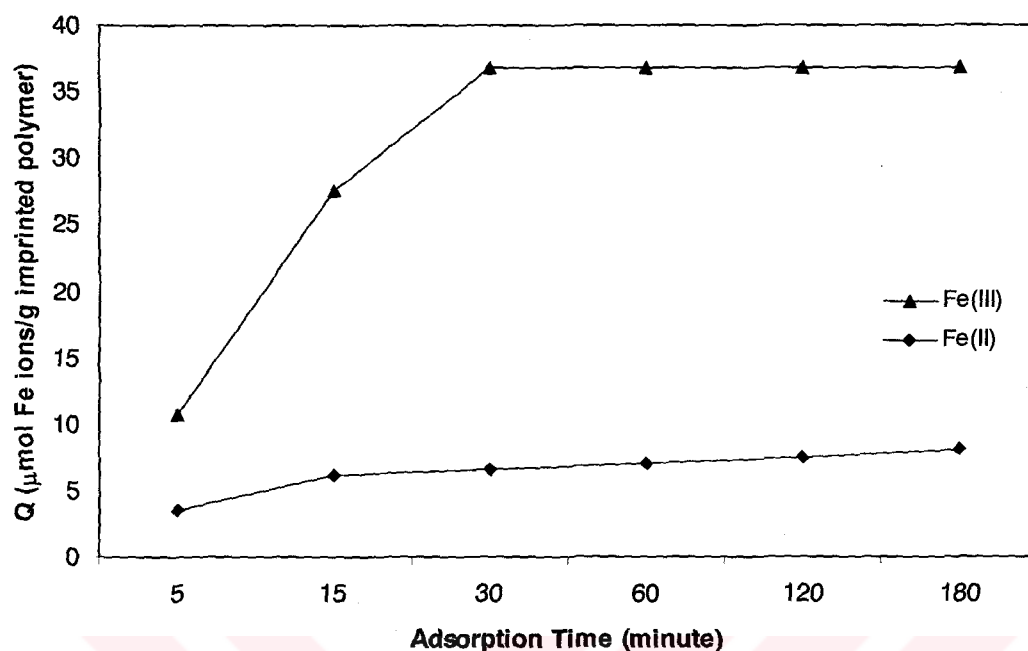


**Figure 4.7.** Time dependent adsorption of  $\text{Fe}^{3+}$  and  $\text{Fe}^{2+}$  ions on the  $\text{Fe}^{3+}$ -imprinted poly(HEMA-co-MAC) beads; initial metal ion concentration:  $5 \text{ mg L}^{-1}$ , pH:3, T:  $25^\circ\text{C}$ .

Several experimental data on the adsorption rates of heavy metal ions by various sorbents have shown a wide range of adsorption time. For example, the adsorption equilibrium time of  $\text{Fe}(\text{III})$ ,  $\text{Fe}(\text{II})$ ,  $\text{Cu}(\text{II})$  and  $\text{Ni}(\text{II})$  on the ethylenediamine functionalized polyacrylamide resin was 5 hour (Latha et al., 1991). Akerkar et al. have investigated  $\text{Mn}(\text{II})$ ,  $\text{Fe}(\text{III})$ ,  $\text{Co}(\text{II})$ ,  $\text{Ni}(\text{II})$ ,  $\text{Cu}(\text{II})$ , and  $\text{Zn}(\text{II})$  adsorption on  $\alpha$ -nitroso- $\beta$ -naphthol resin and reported 24 hour equilibrium adsorption time for batch experiments (Akerkar et al., 1998). Jose and Pillai reported that 9 hours for complexation of amino resin and metal salt solutions (Jose and Pillai, 1996). There are several parameters which determine the adsorption rate in adsorption process, such as structural properties of adsorbent, metal ion properties, stirring rate in the batch set-up or flow rate in column system, the existence of other heavy metal ions or anions. All individual experimental studies published in the literature have been performed under



different conditions; consequently, it is not reasonable to make comparisons of the adsorption rates reported. However, the adsorption rates obtained with the  $\text{Fe}^{3+}$ -imprinted p(HEMA-co-MAC) beads produced by us seem to be very fast. The results provide very useful information for optimizing the  $\text{Fe}^{3+}$  ions binding efficiency of the beads.

#### 4.2.3. Adsorption Capacity

$\text{Fe}^{3+}$  and  $\text{Fe}^{2+}$  ions adsorption capacities of the  $\text{Fe}^{3+}$ -imprinted p(HEMA-co-MAC) beads are presented as a function of the initial concentration of metal ions within the aqueous adsorption medium in Figure 4.8. These batch experiments were performed by using single solutions of the interested ions.  $\text{Fe}^{3+}$  adsorption capacity of the  $\text{Fe}^{3+}$ -imprinted p(HEMA-co-MAC) beads increased first with the increasing of initial concentration of  $\text{Fe}^{3+}$  then reached a plateau value at about an initial  $\text{Fe}^{3+}$  concentration of  $40 \text{ mg L}^{-1}$ . The maximum adsorption capacities of  $\text{Fe}^{3+}$ -imprinted p(HEMA-co-MAC) beads are  $107.7 \text{ }\mu\text{mol}$  and  $32.8 \text{ }\mu\text{mol}$  per gram of the sorbent for  $\text{Fe}^{3+}$  and  $\text{Fe}^{2+}$ , respectively. It should be noted that  $\text{Fe}^{3+}$ -imprinted p(HEMA-co-MAC) beads have a significantly higher selectivity for  $\text{Fe}^{3+}$  than  $\text{Fe}^{2+}$ .

Note that in the absence of complexing agents, the hydrolysis and precipitation of metal ions are affected by the concentration and form of soluble metal species (Reed and Matsumoto, 1993) (Reed and Nonavinakere, 1992) (Boomhower, 1982). The solubility of the metal ion is governed by hydroxide or carbonate concentration; in order to eliminate the effects of precipitation we performed these groups of experiments at pH: 3 for  $\text{Fe}^{3+}$ .

These adsorption capacity values are most probably due to high complexation rate (high affinity) between  $\text{Fe}^{3+}$  ions and template groups in the microbeads structure.



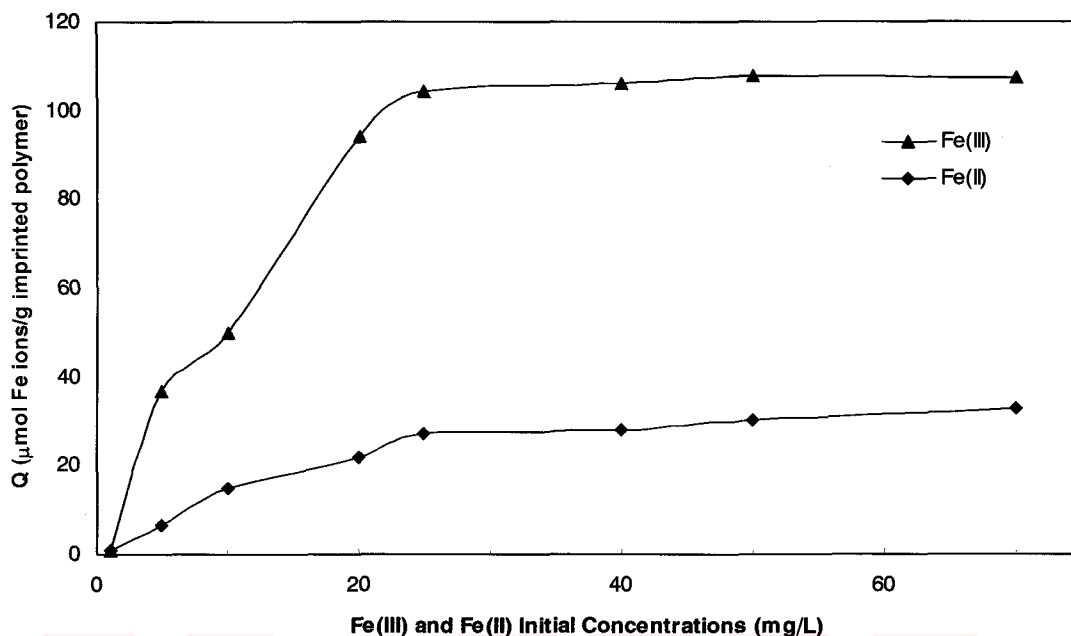


**Figure 4.8.** Adsorption capacity of  $\text{Fe}^{3+}$  and  $\text{Fe}^{2+}$  ion concentration on adsorption of metal ions on the  $\text{Fe}^{3+}$ -imprinted poy(HEMA-co-MAC) beads; pH:3, T: 25°C.

In the previously published papers, capacity of 2- Mercaptobenzimidazole loaded on silica gel (MBI-SG) sorbent for  $\text{Fe}^{3+}$  was found as 500  $\mu\text{g}$  of iron per gram of sorbent (Bagheri et al., 2000). Feng and co-workers used various iron chelating resins for removal of  $\text{Fe}^{3+}$  ions from plasma. DFO-Sepharose, HMP-Sepharose, AHMP-HEMA and AHMP-DMAA resins iron capacities were reported 14.4  $\mu\text{mol}$ , 6.1  $\mu\text{mol}$ , 5.4  $\mu\text{mol}$  and 6.1  $\mu\text{mol}$ , respectively (Feng et al., 1994)

#### 4.2.4. Competitive Adsorption

In order to determine the selectivity of  $\text{Fe}^{3+}$ -imprinted p(HEMA-co-MAC) beads, competitive adsorption of  $\text{Fe}^{3+}/\text{Fe}^{2+}$ ,  $\text{Fe}^{3+}/\text{Cr}^{3+}$ ,  $\text{Fe}^{3+}/\text{Cu}^{2+}$ , and  $\text{Fe}^{3+}/\text{Zn}^{2+}$  from their binary solutions was investigated. Solutions containing 25  $\text{mg L}^{-1}$  of metal ions were treated with 50  $\text{mg}$  of  $\text{Fe}^{3+}$ -imprinted p(HEMA-co-MAC) beads, for 30 minutes at pH 3.

The distribution coefficient ( $K_d$ ) gives the ratio of the amount of metal ion adsorbed by 1 g of the adsorbent to the amount of metal ion remained in 1 mL of the solution and distribution ratio ( $k$ ) indicates the strength of metal-binding by adsorbent. Adsorption capacities,  $K_d$  and  $k$  values are given in Table 4.2.

**Table 4.1.** The effect of imprinting on selectivity

Metal ions	Adsorbed metal ions <sup>c</sup> (mg/g)	$K_d$ (mL/g)	$k$
Fe(III)	5.8 <sup>b</sup>	552.4	
Fe(II) <sup>a</sup>	1.1	50.5	10.9
Cr(III)	1.2	54.5	10.1
Cu(II)	--	--	$\geq K_d$
Zn(II)	--	--	$\geq K_d$

<sup>a</sup> Spectrophotometric 1,10-Phenanthroline method was used determination of  $Fe^{2+}$  concentration in  $Fe^{3+}/Fe^{2+}$  mixture (Vogel, 1986).

<sup>b</sup> The same value was obtained all the experiments.

<sup>c</sup> Each experiment was repeated three times.

It should be noted that the adsorbed value of  $Fe^{3+}$  ions in single solution (corresponding a  $25 \text{ mg L}^{-1} Fe^{3+}$  initial concentration) is  $6.01 \text{ mg g}^{-1}$ . It can be seen (Table 4.2.) that the equilibrium binding capacity of  $Fe^{3+}$  ion was reduced by 3% in the presence of an equal concentration of another metal ions; in the other words, these metal ions slightly inhibit the complexation between  $Fe^{3+}$  ions and template groups in the beads structure. The  $K_d$  value of  $Fe^{3+}$  is very high compared to those of other metal ions. Although  $Cr^{3+}$  ion has same oxidation state as  $Fe^{3+}$ , the  $Fe^{3+}$ -imprinted p(HEMA-co-MAC) beads showed excellent selectivity for the  $Fe^{3+}$  ions. This means that  $Fe^{3+}$  can be determined even in the presence of  $Fe^{2+}$ ,  $Cr^{3+}$ ,  $Cu^{2+}$  and  $Zn^{2+}$  interferences. This shows, the chemical

nature of the template groups in the beads is great importance for the adsorption process.

#### 4.2.5. Interfering ions

The effects of interfering ions have also been studied. Sample solutions containing 5 mg L<sup>-1</sup> of Fe<sup>3+</sup> ions and various amounts of Na<sup>+</sup>, Mg<sup>2+</sup> and Ca<sup>2+</sup> ions as interferants were examined by the general procedure. The chloride, nitrate, carbonate ions are found to be present in natural water and have the capability to complex with many metal ions. Consequently they may reduce the adsorption of metal ions. Thus the effect of NaCl, KCl, Mg(CO<sub>3</sub>)<sub>2</sub> and Ca(NO<sub>3</sub>)<sub>2</sub> on the adsorption of Fe<sup>3+</sup> ions on the Fe<sup>3+</sup>-imprinted p(HEMA-co-MAC) beads was studied under the optimum conditions. Interfering ions effect on Fe<sup>3+</sup> ions adsorption onto Fe<sup>3+</sup>-imprinted (HEMA-co-MAC) beads was shown in Figure 4.9.

The tolerance limit was set as the amount of interfering ion required to cause 3% error in the adsorption of Fe<sup>3+</sup> ions. The results obtained are given in Table 4.2.

**Table 4.2.** Tolerance limit of interfering species

<u>Interfering species</u>	<u>Tolerance limit(mg/L)</u>
NaCl	1500
KCl	800
Mg(CO <sub>3</sub> ) <sub>2</sub>	500
Ca(NO <sub>3</sub> ) <sub>2</sub>	1000

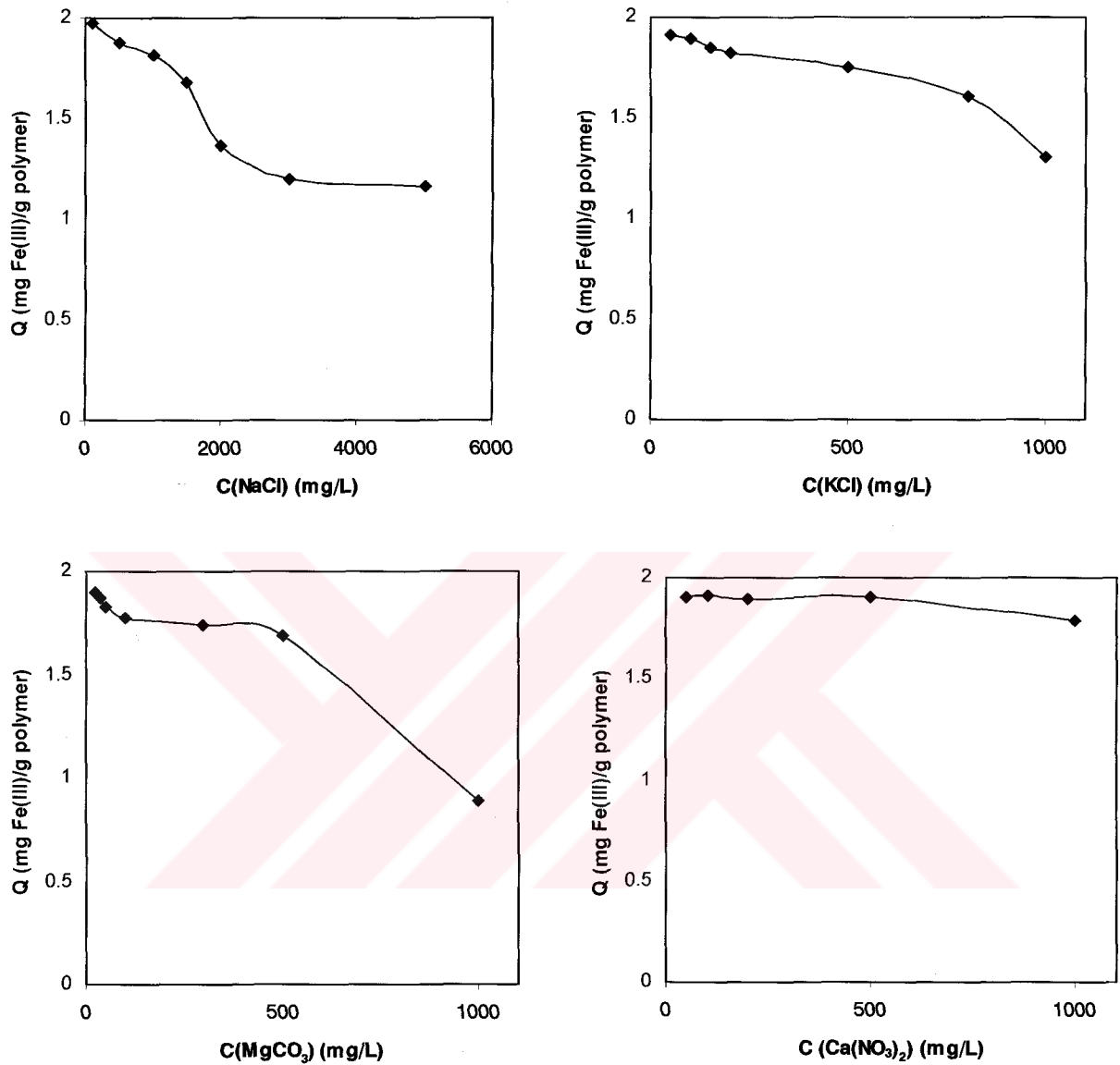


**Figure 4.9.** The effect of NaCl, KCl, Mg(CO<sub>3</sub>)<sub>2</sub> and Ca(NO<sub>3</sub>)<sub>2</sub> on the adsorption of Fe<sup>3+</sup> ions on the Fe<sup>3+</sup>-imprinted p(HEMA-co-MAC) beads, Fe<sup>3+</sup> metal ions initial concentration: 5 mg L<sup>-1</sup>, adsorption time: 30 min., T: 25°C.

#### 4.2.6. Equilibrium studies

The case of sorption process considered here involves a solid phase (sorbent) and a liquid phase (solvent, normally water) containing dissolved species to be

sorbed (sorbate, e.g. metal ions). Due to higher 'affinity' of the sorbent for the sorbate species the latter is attracted into the solid and bound there by different mechanisms. This process takes place until an equilibrium is established between the amount of solid-bound sorbate species and its portion remaining in solution (at a residual, final or equilibrium concentration  $C_f$ ). The degree of the sorbent 'affinity' for the sorbate determines its distribution between the solid and liquid phases.

The quality of the sorbent material is judged according to how much sorbate it can attract and retain in an 'immobilized' form. For this purpose it is customary to determine the metal uptake ( $q$ ) by the sorbent as the amount of the sorbate bound by the unit of solid phase (by weight, volume, etc.).

Since sorption process tends to be exothermic and since the sorption performance may vary with temperature, constant temperature during the sorption process is a basic requirement. Sorption isotherms are plots between the sorption uptake ( $q$ ) and the final equilibrium concentration of the residual sorbate remaining in the solution ( $C_f$ ). This simple relationship can be expressed in slightly different variations.

Sorption is not necessarily so strongly exothermic as other physical adsorption reactions. The temperature range for sorption applications is considered relatively narrow, roughly between (10-70)°C, diminishing thus the temperature sensitivity issue to a large degree.

The  $q$  vs  $C_f$  sorption isotherm relationship can also be mathematically expressed. This was done already in the 1900's in the classical work of Langmuir (Langmuir, 1918) and Freundlich (Freundlich, 1907) who studied activated carbon adsorption. The Langmuir isotherm considers sorption is a chemical phenomenon. It was first theoretically examined in the adsorption of gases in the solid surfaces. Langmuir constant  $b = 1/K$  which is related to the energy of

adsorption through the Arrhenius equation. The higher  $b$  and the smaller  $K$ , is the affinity of the sorbent for the sorbate.  $q_{\max}$  can also be interpreted as the total number of binding sites that are available for sorption, and  $q$  as the number of binding sites that are in fact occupied by the sorbate at the concentration  $C_f$ .

The most widely used isotherm equation for modelling equilibrium data is Langmuir equation, which for dilute solutions may be represented as:

$$q_e = K_L C_e / (1 + a_L C_e) \quad (4.1)$$

The constants  $K_L$  and  $a_L$  are the characteristics of the Langmuir equation and can be determined from a linerized form of the above equation:

$$C_e/q_e = (1/K_L) + (a_L/K_L)C_e \quad (4.2)$$

Therefore, a plot of  $C_e/q_e$  versus  $C_e$  gives a straight line of slope  $a_L/K_L$ . The constant  $K_L$  is the Langmuir equilibrium constant and the ratio  $a_L/K_L$  gives the theoretical monolayer saturation capacity. The Langmuir equation is applicable to homogeneous sorption where each metal ion-imprinted bead sorption process has equal sorption activation energy.

The Freundlich expression is an empirical equation based on sorption on a heterogeneous surface. The Freundlich equation is commonly presented as:

$$q_e = a C_e^b \quad (4.3)$$

and the equation may be linerized by taking logarithms:

$$\ln q_e = b \ln C_e + \ln a \quad (4.4)$$

therefore, a plot of  $\ln q_e$  versus  $\ln C_e$  enables the constant  $a$  and exponent  $b$  determined.

The parameter  $a$  is equivalent to  $q_{\max}$  in the Langmuir isotherm. The Freundlich isotherm does not predict saturation of the solid surface by the adsorbate, thus infinite surface coverage is predicted mathematically.

The Langmuir and Freundlich constants along with the correlation coefficients ( $R^2$ ) have been calculated from the corresponding plots (Figure 4.10.) for  $\text{Fe}^{3+}$  ions on the sorption of  $\text{Fe}^{3+}$ -imprinted p(HEMA-co-MAC) beads and the results are presented in Table 4.3.

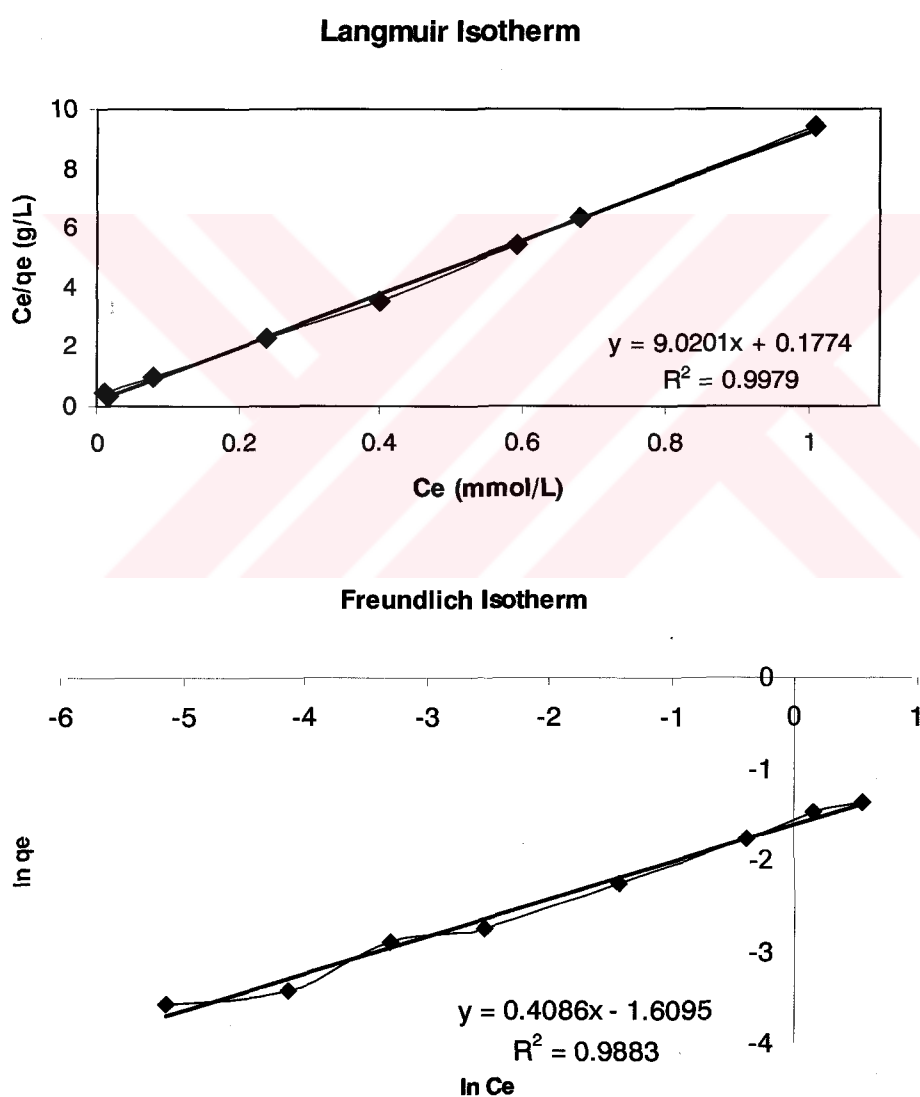


**Figure 4.10.** Langmuir and Freundlich adsorption isotherms.

**Table 4.3.** Isotherm model constants and correlation coefficients for sorption of Fe<sup>3+</sup> ions.

Sorbent	Langmuir			Freundlich		
	$a_i/K_L$ (mg g <sup>-1</sup> )	$K_L$ (10 <sup>3</sup> ) (mol L <sup>-1</sup> )	$R^2$	a	b	$R^2$
Fe <sup>3+</sup> -imprinted (pHEMA-co-MAC)	6.16	100.5	0.9979	0.2	0.4086	0.9883

The correlation regression coefficients show that the adsorption process can be well defined by the Langmuir equation. The Langmuir fit is considered to be evidence that sorption stops at monolayer, consistent with specific and strong sorption onto specific sites. Since the exchange reaction between surface sites previously adsorbed ions is of only a monolayer or less, there is an accumulation of matter at the solid-solution interface without the creation of a three-dimensional (3-D) structure.

Although the Langmuir model sheds no light on the mechanistic aspects of sorption, it provides information on uptake capabilities and is capable of reflecting the usual equilibrium sorption process behaviour. Langmuir assumed that the forces that are exerted by chemically unsaturated surface atoms (total number of binding sites) do not extend further than the diameter of one sorbed molecule and therefore sorption is restricted to monolayer. In the simplest case the following assumptions were made:

- Fixed number of adsorption sites; at equilibrium, at any temperature and gas pressure a fraction of the surface sites  $\theta$  is occupied by adsorbed molecules, and the fraction  $1-\theta$  is free.
- All sorption sites are uniform (i.e. constant heat of adsorption)
- Only one sorbate
- One sorbate molecule reacts with one active site
- No interaction between sorbed species.



As long as its restrictions and limitations are clearly recognized, the Langmuir equation can be used for describing equilibrium conditions for sorption behaviour in different sorbate-sorbent systems, or for varied conditions with in any given system.

### 4.3. Desorption and Reuse

Desorption of the adsorbed  $Fe^{3+}$  ions from the  $Fe^{3+}$ -imprinted p(HEMA-co-MAC) beads was also studied in a batch experimental set-up. Various concentration of HCl,  $HNO_3$ , EDTA and  $NH_4SCN$  were compared for desorption of  $Fe^{3+}$  ions from the imprinted beads after the adsorption step. The desorption ratios of  $Fe^{3+}$  ions were not quantitative with  $NH_4SCN$  and EDTA solutions. It was seen that  $Fe^{3+}$  ions could be effectively desorbed with 20 mL of 0.1 M HCl and 0.1 M  $HNO_3$  and desorption ratios greater than 96.2% and 95.5% respectively. In this study, the desorption time was found to be 30 minutes.

**Table 4.4.** Desorption agents for used  $Fe^{3+}$  ions from the  $Fe^{3+}$ -imprinted p(HEMA-co-MAC).

Desorption Reagents	0.1 M HCl	0.1 M $HNO_3$	0.1 M EDTA	0.1 M $NH_4SCN$
	% 96.2	% 95.5	%63.4	% 56.71

In order to obtain the reusability of the  $Fe^{3+}$ -imprinted p(HEMA-co-MAC) beads, adsorption-desorption cycle was repeated five times by using the same imprinted microbeads. The results showed that  $Fe^{3+}$ -imprinted p(HEMA-co-MAC) beads could be repeatedly used in  $Fe^{3+}$  adsorption without any detectable loss in the initial adsorption capacity.

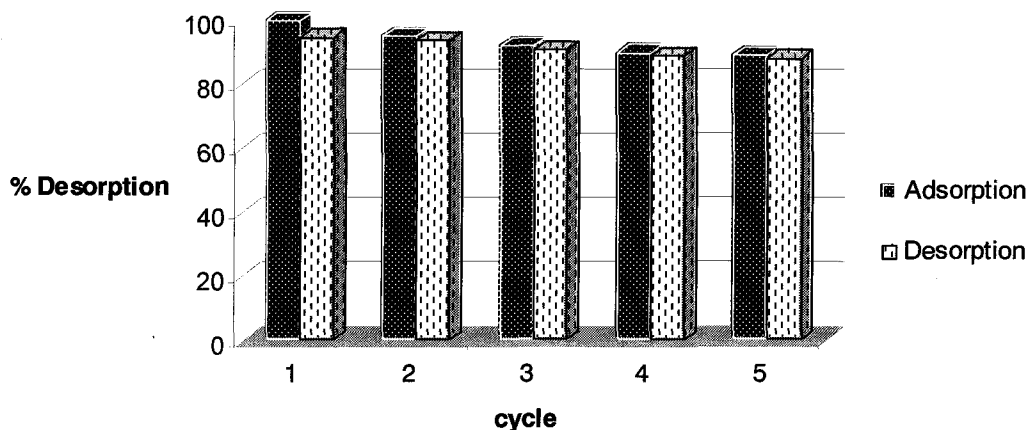


**Figure 4.11.** Adsorption/Desorption cycle of Fe<sup>3+</sup>-imprinted p(HEMA-co-MAC). Desorption agent 0.1 M HCl. In adsorption process, optimum conditions were used, initial concentration of metal ion: 5 mg L<sup>-1</sup>.

#### 4.4. Removal of Fe<sup>3+</sup> ions from Tap-water and Certified Reference Serum

In order to estimate the accuracy of the procedure, different amounts of the Fe<sup>3+</sup> ions were spiked in tap water. 20 mL sample solution was treated under the general adsorption-desorption procedure. The results reported in Table 4.6. A good agreement was obtained between the added and measured analyte amounts.

**Table 4.5.** Removal of Fe(III) ions from tap water (N = 5)

Iron added ( $\mu\text{g mL}^{-1}$ )	Iron found ( $\mu\text{g mL}^{-1}$ )	Recovery (%)
0.00	$0.062 \pm 0.002$	-
2.50	$2.41 \pm 0.11$	96
5.00	$4.86 \pm 0.17$	97

Removal of  $\text{Fe}^{3+}$  ions from certified reference serum sample (SERO 201405-Seronorm Trace Elements Serum, Level 1) and real serum sample with using  $\text{Fe}^{3+}$ -imprinted p(HEMA-co-MAC) beads was also investigated. This reference material is produced from serum collected from thoroughly controlled voluntary blood donors of a Scandinavian blood bank. Each unit separately controlled and found negative for HBS antigen and HIV I, II and hepatitis C antibodies. No preservatives are added to the samples. Contains all normal constituents which ensure the control and test samples to be analysed under the same conditions.

**Table 4.6.** Certified values of reference serum sample.

Element	Certified value in $\mu\text{g L}^{-1}$	Element	Certified value in $\text{mg L}^{-1}$
Al	122	Ca	106
Cr	1.0	Cu	1.2
Co	1.0	Fe	1.25
F	75	Li	5.5
Au	460	Mg	20
Mn	10.6	P	75
Ni	5.5	K	152
Se	83	S	1050
		Na	3373
		Zn	1.33

In order to investigate the removal of  $\text{Fe}^{3+}$  ions from the serum,  $\text{Fe}^{3+}$ -imprinted p(HEMA-co-MAC) beads were used for serum samples containing different amounts of  $\text{Fe}^{3+}$  ions. For unpoisoned serum (iron content in this case was  $1.25 \text{ mg L}^{-1}$ ), and different amount of  $\text{Fe}(\text{NO}_3)_3 \cdot 9\text{H}_2\text{O}$  added ( $1.25, 4.00 \text{ mg L}^{-1}$ ) serum samples was treated with  $\text{Fe}^{3+}$ -imprinted p(HEMA-co-MAC) beads.

**Table 4.7.** Removal of Fe<sup>3+</sup> ions in certified reference serum and real serum sample.

	Certified values (mg L <sup>-1</sup> )	Found (mg L <sup>-1</sup> )	Added (mg L <sup>-1</sup> )	Iron removal <sup>c</sup> (%)
SERO 201405	1.25±0.1 <sup>a</sup>	-	-	30
		-	1.25	35
		-	4.00	37
Real serum sample	-	10.12±1.5 <sup>b</sup>	-	34
		10.84±1.7 <sup>b</sup>	-	32

<sup>a</sup> ICP-AES<sup>b</sup> FAAS<sup>c</sup> Mean value of three determinations.

The results of removal of Fe<sup>3+</sup> ions from certified reference serum sample and real serum sample were shown in Table 4.7. Fe<sup>3+</sup>-imprinted p(HEMA-co-MAC) beads have shown relatively close performance during the treatment with certified reference serum sample and real serum sample. It is known that the iron in plasma is tightly bound to its transport protein, transferrin. Normal serum iron levels fluctuate around 1 mg L<sup>-1</sup>, and typically only 30% iron binding sites of transferrin are occupied, making the total iron binding capacity (TIBC) 3 mg L<sup>-1</sup>. From the results shown in Table 4.7., it can be seen that for unpoisoned serum (iron content in this case was 1.25 mg L<sup>-1</sup>) only a small amount of iron was removed, while more iron was removed at higher iron concentrations. It is interesting to note that the iron content of the treated serum was 0.875 mg L<sup>-1</sup>, this value is the region of normal serum iron level.

In addition, the overloaded iron was removed by the Fe<sup>3+</sup>-imprinting p(HEMA-co-MAC) beads. As a result, the adsorption capacity of Fe<sup>3+</sup>-imprinting p(HEMA-co-MAC) beads was close to adsorption capacity of beads in non-interfering medium.

Mass of polymer is very important parameter in adsorption experiments. It should be noted that affinity will be increased by increasing mass of polymer.

## 5. CONCLUSION

- ✦ pHEMA beads containing MAC metal complexing ligand and/or comonomer, which was prepared and was applied to the selective removal of  $\text{Fe}^{3+}$  ions from aqueous solutions. This novel approach for the preparation of adsorbent has many advantages over conventional techniques; those need the activation of the matrix for metal-complexing ligand immobilization. In this procedure, MAC acts as the metal complexing ligand, and no need to activate the matrix for the metal-complexing ligand immobilization. MAC is polymerized with HEMA and no leakage of the metal-complexing ligand is observed.
- ✦ The suspension polymerization procedure provided cross-linked  $\text{Fe}^{3+}$ -imprinted p(HEMA-co-MAC) beads, which were spherical in shape with a size range of 150-200  $\mu\text{m}$  in diameter mostly. Specific surface area of  $\text{Fe}^{3+}$ -imprinted p(HEMA-co-MAC) beads was found to be  $18.9 \text{ m}^2 \text{ g}^{-1}$ .
- ✦ The equilibrium swelling ratios of  $\text{Fe}^{3+}$ -imprinted p(HEMA-co-MAC) beads used in this study, which were prepared with the recipe given in Table 3.1. was 72%.
- ✦ Due to the elemental analysis results,  $\text{Fe}^{3+}$ -imprinted p(HEMA-co-MAC) beads have approximately  $3.9 \text{ mmol MAC g}^{-1}$  from the nitrogen stoichiometry.
- ✦ Optical photographs and scanning electron micrographs showed that the  $\text{Fe}^{3+}$ -imprinted p(HEMA-co-MAC) beads have a microporous interior surrounded by a reasonable rough surface, in dry state. The roughness of the beads surface should be considered as a factor providing an increase in surface area.

- ✚ In equilibrium adsorption time studies, high adsorption rates were observed at the beginning, and then plateau values were gradually reached within 5-30 min for adsorption of  $\text{Fe}^{3+}$  and  $\text{Fe}^{2+}$  ions on the beads. The maximum adsorption capacity for  $\text{Fe}^{3+}$  and  $\text{Fe}^{2+}$  ions were 107.7  $\mu\text{mol}$ , 32.8  $\mu\text{mol}$  per gram dry weight of beads, respectively. The fast adsorption equilibrium is most probably due to the high complexation and geometric affinity between  $\text{Fe}^{3+}$  ions and  $\text{Fe}^{3+}$  cavities in the beads structure.
- ✚ The adsorption values increased with increasing concentration of  $\text{Fe}^{3+}$  ions, and a saturation value is achieved at ion concentration of 40  $\text{mg L}^{-1}$ , which represents saturation of the active binding cavities on the  $\text{Fe}^{3+}$ -imprinted p(HEMA-co-MAC) beads.
- ✚ A comparison of the  $K_d$  values, it can be seen that the equilibrium binding capacity of  $\text{Fe}^{3+}$  ion was reduced by 3% in the presence of an equal concentration of another metal ions ( $\text{Cr}^{3+}$ ,  $\text{Fe}^{2+}$ ,  $\text{Cu}^{2+}$ ,  $\text{Zn}^{2+}$ ) in the other words, these metal ions slightly inhibit the complexation between  $\text{Fe}^{3+}$  ions and template groups in the beads structure. The  $K_d$  value of  $\text{Fe}^{3+}$  is very high compared to those of other metal ions.
- ✚ The effects of interfering ions of NaCl, KCl,  $\text{Mg}(\text{CO}_3)_2$  and  $\text{Ca}(\text{NO}_3)_2$  on the adsorption of  $\text{Fe}^{3+}$  ions on the  $\text{Fe}^{3+}$ -imprinted p(HEMA-co-MAC) beads were found that, 1500, 800, 500, 1000 in tolerance limit, respectively. The tolerance limit was set as the amount of interfering ion required to cause 3% error in the adsorption of  $\text{Fe}^{3+}$  ions.
- ✚ The maximum adsorption capacity ( $q_{\text{max}}=6.16 \text{ mg g}^{-1}$  beads) for the adsorption of  $\text{Fe}^{3+}$  ions was obtained from the experimental data. The correlation regression coefficient 0.9979 shows that the adsorption process can be well defined by the Langmuir equation.

- ✦ The desorption time was found to be 30 min. Desorption ratios were high (up to 96.2%). In order to obtain the reusability of the  $\text{Fe}^{3+}$ -imprinted p(HEMA-co-MAC) beads, adsorption-desorption cycle was repeated five times by using the same imprinted microbeads. The results showed that  $\text{Fe}^{3+}$ -imprinted p(HEMA-co-MAC) beads could be repeatedly used in  $\text{Fe}^{3+}$  adsorption without any detectable loss in the initial adsorption capacity.
- ✦ In order to estimate the accuracy of the procedure, different amounts of the  $\text{Fe}^{3+}$  ions were spiked in tap water. 20 mL sample solution was treated under the general adsorption-desorption procedure. Recovery results were found %97 approximately. In order to determine the removal of  $\text{Fe}^{3+}$  ions from the serum,  $\text{Fe}^{3+}$ -imprinted p(HEMA-co-MAC) beads were used for serum samples containing different amounts of  $\text{Fe}^{3+}$  ions. The  $\text{Fe}^{3+}$ -imprinted p(HEMA-co-MAC) beads removed 33%  $\text{Fe}^{3+}$  ions from reference serum and real serum samples.

## REFERENCES

- Acheterberg, E.P., Holland, T.W., Bowie, A.R., Mantoura, R.F.C., Worsfold, P.J., 2001, Determination of iron in seawater. 442, 1-14.
- Adleman, R., Saul, R.L., Ames, B.N., 1988. Proc. Natl. Acad. Sci. USA. 85, 2706-2708.
- Akerkar et al., 1998. Talanta 46,1461-1467.
- Akl, M.A., 2003. J. Microchem. 75, 1999.
- Alexander, C., Smith, C., Whitcombe, M.J., Vulfson, E.N., 1999. J. Anal. Chem. Soc. 123, 12420-12421.
- Ames, B.N., Shigenaga, M.K., Hagen, T.M., 1993 . Proc. Natl. Acad. Sci. USA. 90, 7915-7922.
- Andersson, L.I., 2000. J. Chromatogr. B. 739, 163-173.
- Andersson, L.I., Paprica, A., Arvidsson, T., 1997. Chromatographia. 46, 57-62.
- Anderson, J., 1974. At. Absorption Newslett. 13, 31.
- Anke, M., 1961\1962, Arch. Tierenahr. 16, 199-123.
- Anke, M., 1966, Arch. Tierernahr. 16, 199-213.
- Anke, M., Flachowsky, G., Henning, A., Partschefeld, M., 1975 . Karl-Marx Univ. Leipzig, 309-319.
- Anke, M., Grun, M., Partschefeld, M., 1976. Hemphill, D.D. (ed), Univ., Missouri, Columbia, USA. 10, 403-409.
- Anke, M., Klinger, G., Grun, M., Krause, G., 1980, Gesundheitswesen. 35, 1967-1972.
- Anke, M., 1986, Lebensmitteltoxikologie. Macholz, R., Lewerenz, H.J. (eds), Akademie-Verlag Berlin, im Druck.
- Ariza, M.E., Bijur, G.N. and Williams, M.V., 1998. Environ. Mol. Mutagen. 31, 352-361.
- Atsui, J., Higashi, M., Takeuchi, T. 2000. J. Am. Chem. Soc. 122, 5218-5219.
- Aurand, K., Blei und Umwelt, Verein für Wasser-, Boden- und Luftthygiene, Berlin, p.5.



- Bae, S.Y., Sauthard, G.L., Murray, G.M., 1999. *Anal. Chim. Acta.* 397, 173.
- Bagheri H., Gholami A., Najafi A., 2000. *Anal. Chim. Acta.* 424, 233-242.
- Barbeau, K., Moffett, J.W., Caron, D.A., Croot, P.L., 1996. *Nature.* 380, 61.
- Baruah, K.M. and Gogoi, P.C., 1998. *Fuel*, 77, 9/10, 979-985.
- Baynes, J.W., 1996. *Diabetes.* 40, 405-411.
- Berman, E., 1967. *At. Absorption Newslett.* 6, 57.
- Bindra, G.S., Gibson, R.S., B., 1985. Mills, C.F., Bremner, I., Chesters, J.K., (eds). *Commonwealth Agricultural Bureaux U.K.* 5, 779-781.
- Bokowski, D.L., 1968. *Am. Indust. Hygn. Assn. J.* 29, 474.
- Bradbear, R.A., Bain, C., Siskind, V., Schofield, F.D., Webb, S., Azelsan, E.M., Halliday, J.W., Basset, M.L. and Powell, L.W., 1985. *J. Natl. Cancer Inst.* 75, 81-84.
- Bray, W.C. and Gorin, M.H., 1932. *J. Am. Chem. Soc.* 54, 2124-2125.
- Bukenberger, U., Lodemann, C. K. W., Loezchke, J., 1972. *Oberrhein. Geol. Abh.* 21, 43.
- Campenhausen, H., and Muller-Plathe, O., 1975. *Z. Klin. Chem. Klin. Biochem.* 13, 489.
- Carter, D.E., 1995. *Environ. Health Perspect.* 103 (supp 1): 17-29.
- Cernik, A.A. and Sayers, M.H.P., 1971. *Brit. J. Industr. Med.* 28, 392.
- Cerutti, P.A., 1985. *Science.* 268, 375-381.
- Cerutti, P.A. and Trump, B.F., 1991. *Cancer Cells.* 3, 1-7.
- Cerutti, P.A., Ghosh, R., Oya, Y., Amstad, P., 1994. *Environ. Health Perspect.* 102 (suppl 10), 123-130.
- Chianella, I.; et al. 2002. *Anal. Chem.* 74, 1288-1293.
- Crichton, R.R., Chaloteaux-Waters, C., 1987. *Eur. J. Biochem.* 164, 485-506.

- Cotran, R.S., Kumar, V., Robbins, S.L., 1989, In Robbin's Pathological Basis of Disease 5<sup>th</sup> edition. W.B. Saunders Philadelphia PA. 861-863.
- Cotton, F.A., Wilkinson, G., 1988. Wiley, New York.
- Coup, M.R., Campell, A.G., 1964, N.Z.J. Agric . Res. 7, 624-630.
- Cross, C.E., Halliwell, B., Borish E.T., Pryor, W.A., Ames, B.N., Saul, R.N., McCord J.M., Harman, D., 1987, Oxygen radicals and human disease. Ann. Int. Med. 107, 526-545.
- Dai, S., Burleig M.C., Shin Y., Morrow C.C., Barnes C.E., 1999. Angew. Chem., Int. Ed. Engl. 38, 1235.
- Denizli, A., Tanyolaç, D., Özdural, A., 1999. J. Chromatogr. A. 793, 47.
- Donaldson, W.E. and Knowles S.O., 1993. Comp. Biochem. Physiol. 104C, 377-379.
- Fanto, J.C. and Ward, P.A., 1982. Am. J. Pathol. 107, 597-418.
- Feng, M., Does van der L., Bantjes, A., 1994. React. Polymers. 23, 63-69.
- Fenton, H.J.H., 1894. J. Chem. Soc. 65, 899-990.
- Floyd, R.A., 1991. Science. 254, 1597.
- Forbes, G., 1947. Brit. Med. J. 1, 367-370.
- Forstner, U. and Muller, G., 1974. Schwermetalle in Flüssen und Seen. Springer-Verlag, Berlin/Heidelberg/ New York.
- Forth, W., Rummel, W., 1984, Allgemeine und spezielle Pharmakologie und Toxikologia, Forth, W., Henscheler, D., Rummel, W. (eds). /Vien/Zurich B.I.-Wissenschaftsverlag.
- Fransson, G.-B., Hoffman, B., Lonnerdal, B., Keen. C.L., 1985. Mills C.F., Bremner, I., Chesters, J.K. (eds). Commonwealth Agricultural Bureaux U.K. 5, 512-515.
- Glaid, J.M., Rao, T.P., 2002. Anal. Lett. 35, 501.
- Gledhill, M., Berg, van den C.M.G., 1995. Mar. Chem. 50, 51.
- Granger, j., Price, N.M., 1999. Limnol. Oceanogr. 44, 541.

- Gruden, N., 1977, *Nutr. Metab.* 21, 305-309.
- Grun, M., Anke, M., Henning, A., Seffner, W., Partschefeld, M., Flachowsky, G., Groppe, B., 1978, *Arch. Tierernahr.* 28, 341-347.
- Gutteridge, J.M.C., 1988. Halliwell, B. (ed). Allen Press, Lawrence, Kansas.
- Gutteridge, J.M.C., Halliwell, B., 1990. *Environ. Health Perspect.* 102 (suppl. 10), 5-12.
- Habermann E., Crowell, K., Janicki, P., 1983 . *Arch. Toxicol.* 54, 61-70.
- Haese, R.R., Wallmann, K., Dahmke, A., 1997. *Geochim. Cosmochim. Acta.* 61, 63.
- Hall, A. and Godinho, M. C., 1980. *Anal. Chim. Acta.* 113, 369.
- Halliwell, B., 1987. *FASEB J.* 1, 358-364.
- Halliwell, B. And Cross, J.K., 1994. *Mutation Res.* 36, 221-228.
- Harmon, B.G., Becker, D.E., Jensen, A.S., Norton H.W., 1968. *J. Animal Sci.* 27, 418-427.
- Haupt, K., Mosbach, K., 2000. *Chem. Rev.* 100, 2495.
- Herrmann, R., Lang, W., Stamm, D., 1965. *Blut.* 11, 135.
- Hong, H.S., Kester, D.R., 1986. *Limnol. Oceanogr.* 31, 512.
- Horbett, T., Brash, J.L., 1987. In *proteins at interfaces physicochemical and biochemical studies.* 1-33.
- Hsing, A.W., McLaughlin, J.K., Olsen, J.H., Mellekjær, L., Wacholder, S. and Fraumeni, J.F., 1995. *Int. J. Cancer.* 60, 160-162.
- Hutchins, D.A., Bruland, K.W., 1994. *Mar. Ecol-Prog. Ser.* 110, 59.
- Hutchins, D.A., Witter, A.E., Butler, A., Luther, G.W., 1999. *Nature.* 400, 858.
- Ielleddi, R., 1997. *Zavod Lab.* 63, 58.
- Jose, L., Pillai, R., 1996. *J.Appl. Poly. Science.* 60, 1855-1865.
- Joyner, T. and Finley, J.S., 1966. *At. Absorption Newslett.* 5, 4.

- Junker-Buchheit, A., Witzenbacher, M., 1996. *J. Chromatogr. A.* 737, 67.
- Kara, D., Alkan, M., 2001. *Talanta.* 55, 415.
- Katz, A., Davis, M.E., 2000. *Nature.* 403, 286-289.
- Kensler, T.W. and Taffe, B.G., 1986. *Adv. Free Radical Biol. Med.* 2, 347-387.
- Kirchgessner, M., Reichlmayr-Lais, A.M., 1981. McC Howell J., Gawthorne, J., White C.L. (eds), *Austral. Acad. Sci. Canberra* 4, 390-393.
- Kma, K., Nishioka, J., Matsunaga, K., 1996. *Limnol. Oceanogr.* 41, 396.
- Knekt, P., Reunanen, H., Takkunen, H., Aroma, A., Heliovara, M. and Hakulinen, T., 1994. *Int. J. Cancer.* 56, 379-382.
- Komiyama, M., Takeuchi, T., Mukawa, T., Asanuma, H., 2002, *Molecular Imprinting: From Fundamentals to Applications.* Wiley-VCH, New York.
- Kristal, B.S. and Yu, B.P., 1992, An emerging hypothesis. *J. Gerontol.* 47, B104-107.
- Kubova, J., Neveral, V., Stresko, J., 1994, *Anal. At. Spectrom.* 9, 241.
- Latha A.G., George B.K., Kannon K.G., Ninan K.N., 1991. *J. Appl. Polym. Sci.* 43, 1159.
- Lave, L.B., Ennever, F.K., 1990, *Annu Rev. Public Health.* 11, 69-87.
- Lawton, L.J. and Donaldson, W.E., 1991. *Biol. Trace Elem. Res.* 28, 83-97.
- Lawlor, N.J., Smith, W.H., Beeson, W.M., 1965, *J. Animal Sci.* 24, 742-749.
- Lehn, J.-M., 1999. *Chem. Eur. J.* 5, 2455-2463.
- Lewis, W.G., et al., 2002. *Angew. Chem. Int. Ed.* 41, 1053-1057.
- Li, J.P. and Chen, Y.J., 1998. *Fenxi Kexue Xuebao.* 14, 148.
- Lloyd, R.V., Hanna, P.M., Mason R.P., 1997. *Free Radical Biol. Med.* 22, 885-888.
- Lossner, G. L., 1978. *At. Absorption Newsslett.* 17, 41.
- Martin, J.H., Gordon, R.M., Broenkow, W.W., 1989. *Fitzwater Deep-Sea Res. Part A.* 36, 649.

- McCord, J.M., 1985. *N. Engl. J. Med.* 312, 159-163.
- Mertz, W., 1981, *Science*. 213, 1332-1336.
- Millero, F.J., Yao, W.S., 1995. *J. Aicher. Mar. Chem.* 50, 21.
- Minezevski, J., Chwastowska, J., Dybezyński, D., 1982. Ellis Horwood, Chichester.
- Mossman, B.T., Bignon, J., Corn, M., Seaton, A. and Gee, J.L.B., 1990. *Science*. 247, 294-301.
- Munger, J.W., Waldman, J.M., Jacob, D.J., Hoffman, M.R., 1983. *J. Geophys. Res.* 88, 5109.
- Nakagawa, K., Harauchi, K., Ogata, T., 1998. *Anal. Sci.* 14, 317.
- Namboothiri, K.K., Baalashubramanian, N., Ramakrishna T.V., 1991. *Talanta*. 38, 945.
- Neidereau, C., Strohmyer, G., 1985. *N. Engl. J. Med.* 313, 1256-1262.
- Nelson, R.G., 1992. *Free Rad. Biol. Med.* 12, 161-168.
- Nelson, R.G., Davis, F.G., Sutter, E., Sobin, L.H., Kikendal, J.W. and Bowen, P., 1994. *J Natl. Cancer Inst.* 86, 455-460.
- Nolting, R.F., Gerringa, L.A., Swagerman, K.R., Timmermans, H.J.W., de Baar, 1998. *Mar. Chem.* 62, 335.
- Obata, H., Karatani, H., Matsui, M., 1997. *Mar. Chem.* 56, 97.
- Ochs, M. and Ivyochs, S., 1997. *Nucl. Instrum. Methods Phys. Res. Sect. B.* 12, 235.
- Olsen, J., Martin, P., Wilson, I. D. 1998. *Anal. Commun.* 35, 13H-14H.
- Olson, A.D. and Hamlin, W.B., 1969. *Clin. Chem.* 15, 438.
- Panasyuk, T.L., Misky, V.M., Piletsky, S.A., Wolfbeis, O.S., *Anal. Chem.* 71, 4609-4613.
- Parker, M.W., Humoller, F.L., Mahler D.J., *Clin. Chem.* 13, 40.
- Pehkonen, S., 1995. *Analyst*, 120, 2655.

- Perez, N., Whitcombe, M.J., Vulfson, E.N., 2001, *Macromolecules*. 34, 830-836.
- Piletsky, S.A., et al., 2000. *Macromolecules*. 33, 3092-3098.
- Pozdniakova, S. and Padaruskas, A., 1998. *Analyst*. 123, 1497.
- Purves, D., 1985. Elsevier Science Publishers BV, Amsterdam.
- Pyrzynska, K., Trojanowicz, M., 1999, *Crit. Rev. Anal. Chem.* 29, 313.
- Qin, W., Zhang, Z.J., Wang, F.C., 1998. *Fresenius J. Anal. Chem.* 360, 130.
- Rahhal, S. and Richter, H.W., 1988. *J. Am. Chem. Soc.* 110, 3126-3133.
- Ramm, G.A., Powell, L.V., Halliday, J.W., 1994. *Hepatology*. 19, 504-513.
- Ramstrom, O., Ye, L., Mosbach, K., 1998. *Anal. Commun.* 35, 9-11.
- Rao, P.T., Preetha, C.R., Separation and purification methods, personal communication.
- Reed, B.E. and Matsumoto M.R., 1993. *Sep. Sci. Technol.* 28, 2179.
- Reed, B.E. and Nonavinakere, S.K., 1992. *Sep. Sci. Technol.* 31, 1985.
- Reinhold, J.G., Pascoe, E., and Kfoury, G.A., 1968. *Anal. Biochem.* 25, 557.
- Riedel, E., Anke, M., Kronemann, H., 1982, *Mengen- und Spurenelemente*. 2, 57-66.
- Ringhardt, I., and Welz, B., 1968. *Z. Anal. Chem.* 243, 190.
- Rue, E.L., Bruland, K.W., 1997. *Limnol. Oceanogr.* 42, 901.
- Saracoglu, S. and Soylak, M., 2001. *Trace Elem. Electrolyt.* 18, 129.
- Saraymen, R. and Soylak, M., 1997. *Int. J. Chem.* 8, 27.
- Sarma, L.S., et al., 2000. *J. Indian Chem. Soc.* 77, 8, 405.
- Saunders, G.D., Foxon, S.P., Walton, M.J., Joyce, S.N., 2000. *Port. Chem. Commun.* 273.
- Say, R., Birlik, E., Ersoz, A., Yilmaz, F., Gedikbey, T., Denizli, A., 2003. *Anal. Chimica Acta*. 1-8.

- Schelenz, R.F.W., Hartmuth-Hoene, A.-E. B., 1985. Mills, C.F., Bremner, I., Chesters, J.K., (eds). Commonwealth Agricultural Bureaux U.K. 5, 620-622.
- Schock, M.R. and Mercer, R. B., 1977. At. Absorption Newslett. 16, 30.
- Schwarz, K., Spallholz, J.E., 1977, Cadmium. Anke, M., Schneider, H.-J. (eds). Spurenelementsymposium 2- Wissenschaftl, Publicationen F.-Schiller- Univ. Jena, 188-193.
- Seligman, P.A., Klausner, R.D., Huebers, H. A., 1987. G. Stamatoyannopoulos, A.W. Nienhuis, P.W. Majerus (eds). W. B. Saunders Philadelphia PA. 219-224.
- Sellergen, B., 2001. Elsevier, Amsterdam.
- Shibata, S., 1961. Anal. Chim. Acta. 25, 1, 348.
- Shigenaga, M.K., Hagen, T.M., Ames, B.N., 1994. Proc. Natl. Acad. Sci. USA. 91, 10771-10778.
- Silva, da J.B.B., Quinaia, S.P., Rollemberg, M.C.E., 2001. Fresenius J. Anal Chem. 369, 657.
- Silverstein, R.M., Bassler, G.C., Morrill, T.C., 1981. Wiley, New York.
- Simonian, N.A. and Coyle, J.T, 1996. Annu. Rev. Pharmacol Toxicol. 36, 83-106.
- Sing, K., 1999. Int. Sugar J. 101, 1211, 554.
- Shvoeva, O.P. and Dedkova, V.P., 1997. J. Anal. Chem. (Transl. of Zh. Anal. Khim. 52, 621.
- Skoog, D.A. and West, 1992. CBS College Publishing, 7<sup>th</sup> Edition. New York.
- Slater, T.F., 1984. Biochem. J. 222, 1-15.
- Soylak, M. and Elci, L., 1997. Int. J. Environ. Anal. Chem. 66, 51.
- Soylak, M., 1998. Fresenius Environ. Bull. 7, 383.
- Stevens, R.G., Garubard, B.I., Micozzi, M.S. and Taylor, P.R., 1994. Int. J. Cancer. 56, 364-369.

- Stevens, R.G., Jones, D.Y., Micozzi, M.S., and Taylor, P.R., 1988. *N. Engl. J. Med.* 319, 1047-1052.
- Stohs, S.J., Bagchi, D., 1995. *Free Radical Bio. Med.* 18, 321-326.
- Sulitzky, C., Ruckert, B., Hall, A.J., Lanza, F., Unger, K., Sellergen, B., 2002. *Macromolecules.* 35, 79-91.
- Surugiu, I., Danielsson, B., Ye, L., Mosbach, K., Haupt, K., 2001. *Anal. Chem.* 73, 487-491.
- Taher, M.A., and Krishan, B., 1995. *Ann. Di Chim.* 85, 3-4, 183.
- Tavenier, P. and Hellendoorn, H.B.A. 1969. *Clin. Chim. Acta.* 23, 47.
- Taylor, S.R., McLennan, S.M., 1985. Blackwell Scientific Publications, London.
- Toyokuni, S., 1996. *Free Radical Biol. Med.*, 20, 553-566.
- Turker, A.R., Bag, H., Erdogan, B., 1997. *Fresenius J. Anal. Chem.* 357, 351.
- Ugo, P., Moretta, L.M., Boni, De A., Scopece, P., Mazzocchin, G.A., 2002. *Anal. Chim. Acta.* 474, 147-160.
- Underwood, E., 1962. Academic Press Inc. New York and London.
- Uzeu, K., Yoshida, M., Goto, M., Furusaki, S., 1999. *Chemtech.* April, 12.
- Vallyathan, V. and Shi, X., 1997. *Environ. Health. Perspect.* 105 (suppl. 1), 165-177.
- Vanderborght, B. M. and van Grieken, R.E., 1977. *Anal. Chem.* 49, 311.
- Vigneau, O., Pinel, C., Lemaire, M., 2002. *Chem. Lett.*, 202.
- Vilatakis, G., Andersson, L., Muller, R., Mosbach, K., 1993. *Nature.* 361, 645-647.
- Vogel's Textbook of Quantitative Inorganic Analysis, 1986. ELBS Publishing.
- Ye, L., Yu, Y., Mosbach, K., 2001. *Analyst.* 126, 760-765.
- Ye, L., Mosbach, K., 2001. *J. Anal. Chem. Soc.* 123, 2901-2902.
- Yilmaz, E., Haupt, K., Mosbach, K., 2000. *Angew. Chem. Int. Ed.* 39, 2115-2118.



Yoshikawa, M., Izumi, J., Kitao, T., Koya, S., Sakamoto, S., 1994. Preprints for the 16<sup>th</sup> Annual Meeting of the Membrane Society of Japan. A1-1-1.

Yu, Y., Ye, L., Haupt, K., Mosbach, K., 2002. *Angew. Chem. Int. Ed.* 41, 4459-4463.

Zaino, E.C., 1967. *At. Absorption Newslett.* 6, 93.

Zettner, A., Sylvia, L.C., Capacho-Delgado, L., 1966. *Am. J. Clin. Pathol.* 45, 533.

Zettner, A. and Mensch, A.H., 1968. *Am. J. Clin. Pathol.* 49, 196.

Warner, H.R., 1994. *Free radical Bio. Med.*, 17, 249-258.

Wenli, L., D'Ascenzo, G., Curini, R., Gasparani, G.M., Casarsi, M., Mattia, B., Traverso, D.M., Bellisario, F., 1998. *Anal. Chim. Acta*, 362, 253.

Wright, T.L., Fitz, J.G., Weisinger, R.A., 1988. *J. Biol. Chem.*, 263, 1842-1847.

Wulff, G., 1995. *Angew. Chem. Int. Ed. Engl.* 34, 1812.

## CURRICULUM VITAE

**Name & Surname** : Özgen SAATÇILAR

**Place of Birth** : Ankara

**Date of Birth** : 23.09.1978

**Marital Status** : Single

### ***Educational and Academic Life***

**High School** : 1993-1995 Çanakkale High School

**B.Sc.** : 1996-2001 Hacettepe University Department of Chemistry

**M.Sc.** : 2001-Hacettepe University Inst. Grad. Stud. In Pure & A

### ***Foreign Language***

English

### ***Work Experience***

March 2004 – December 2004 : Gemsan A.S. R&D and Technical Service Specialist